ESPOO 2008 VTT PUBLICATIONS 701

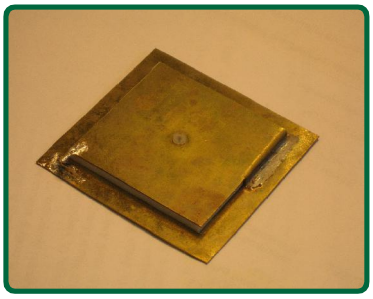

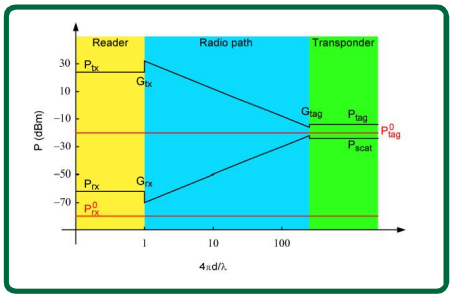


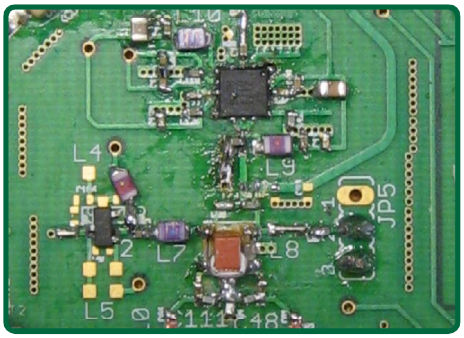


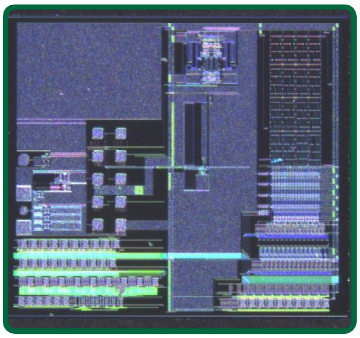

Pekka Pursula

# Analysis and Design of UHF and Millimetre Wave Radio Frequency Identification

VTT PUBLICATIONS 701

# Analysis and Design of UHF and Millimetre Wave Radio Frequency Identification

Pekka Pursula

*Dissertation for the degree of Doctor of Science in Technology to be presented with due permission of the Faculty of Information and Natural Sciences, for public examination and debate in Auditorium AS1, Helsinki University of Technology (Espoo, Finland) on the 30th of January, 2009, at 12 noon.*

ISBN 978-951-38-7133-8 (soft back ed.)
ISSN 1235-0621 (soft back ed.)

ISBN 978-951-38-7134-5 (URL: http://www.vtt.fi/publications/index.jsp)
ISSN 1455-0849 (URL: http://www.vtt.fi/publications/index.jsp)



JULKAISIJA – UTGIVARE – PUBLISHER

VTT, Vuorimiehentie 3, PL 1000, 02044 VTT
puh. vaihde 020 722 111, faksi 020 722 4374

VTT, Bergsmansvägen 3, PB 1000, 02044 VTT
tel. växel 020 722 111, fax 020 722 4374

VTT Technical Research Centre of Finland, Vuorimiehentie 3, P.O. Box 1000, FI-02044 VTT, Finland
phone internat. +358 20 722 111, fax +358 20 722 4374

VTT, Tietotie 3, PL 1000, 02044 VTT
puh. vaihde 020 722 111, faksi 020 722 7012

VTT, Datavägen 3, PB 1000, 02044 VTT
tel. växel 020 722 111, fax 020 722 7012

VTT Technical Research Centre of Finland, Tietotie 3, P.O. Box 1000, FI-02044 VTT, Finland
phone internat. +358 20 722 111, fax +358 20 722 7012

Cover: A platform-tolerant UHF RFID transponder antenna (above left); A power budget diagram of an UHF RFID System (above right); The adaptive RF front end of an EPC Gen2 UHF RFID reader (below left, courtesy of Perlos Corporation); And a UHF RFID transponder IC with a sensor interface (below right).

Edita Prima Oy, Helsinki 2008

Pursula, Pekka. Analysis and Design of UHF and Millimetre Wave Radio Frequency Identification [UHF- ja millimetriaaltoalueen radiotunnistusjärjestelmien tutkimus ja suunnittelu]. Espoo 2008. VTT Publications 701. 82 p. + appendices 51 p.

**Keywords** Radio frequency identification, RFID, ultra high frequency, UHF, millimetre waves, millimetre wave identification, MMID, antenna, scattering, backscattering modulation, scattering measurement, reader device, adaptive rf front end.

# Abstract

Radio frequency identification (RFID) is an asymmetric radio protocol, where uplink communication (from transponder to reader) is implemented with backscattering modulation. The idea was first demonstrated in the 1940's. One of the first consumer applications of RFID was access control, and key cards based on an inductive near field coupling are widely used even today. The introduction of Schottky diodes to CMOS processes enabled passive RFID, i.e. transponders without a battery, at ultra high frequencies (UHF) with reasonable cost and read range in the end of 1990's. This has opened up new applications and inspired new research on RFID.

This thesis studies the radio frequency (RF) components and general RF phenomena in RFID at UHF and millimetre waves. The theoretical analysis of the radio path reveals that the read range of a passive UHF system is ideally limited by the downlink, i.e. the power transfer from reader to the transponder. However, the architecture of the reader RF front end is critical, because the transmitted signal may couple a significant amount of noise to the receiver, overpowering the faint reflection from the transponder. In the thesis, two adaptive RF front ends are introduced to eliminate the noise coupling from the transmitter.

One of the most critical problems with UHF RFID has been the detuning of transponder antennas on different mounting platforms. The detuning may significantly diminish the read range of the transponder, especially on metal surfaces. In this thesis, two backscattering-based measurement techniques for the transponder antennas are presented. The detuning effect has been studied using these measurement techniques, and a platform tolerant-antenna is introduced.

RFID at millimetre waves enables miniaturisation of the reader antenna, and widening the data bandwidth over short distances. This could be used to access wirelessly mass memories with wide data bandwidth. A semi-passive or active transponder could communicate, e.g., with automotive radars. The millimetre wave identification (MMID) has been theoretically studied and experimentally verified at 60 GHz.

Pursula, Pekka. Analysis and Design of UHF and Millimetre Wave Radio Frequency Identification [UHF- ja millimetriaaltoalueen radiotunnistusjärjestelmien tutkimus ja suunnittelu]. Espoo 2008. VTT Publications 701. 82 s. + liitteet 51 s.

**Avainsanat** Radio frequency identification, RFID, ultra high frequency, UHF, millimetre waves, millimetre wave identification, MMID, antenna, scattering, backscattering modulation, scattering measurement, reader device, adaptive rf front end.

# Tiivistelmä

Radiotunnistus (RFID) on lyhyen kantaman radioprotokolla, jossa yksinkertaisen tunnisteen muisti voidaan lukea langattomasti lukijalaitteen avulla. Tiedonsiirto tunnisteesta lukijalaitteeseen perustuu tunnisteen takaisinsironnan moduloimiseen. Tekniikka on osoitettu kokeellisesti toimivaksi jo 1940-luvulla. Radiotunnistuksen ensimmäisiä kuluttajasovelluksia on induktiivisiin kulkukortteihin ja lukulaitteisiin perustuva kulunvalvonta, jota käytetään tänäkin päivänä yleisesti. Passiivisten, eli paristottomien, tunnisteiden valmistaminen UHF-taajuusalueelle halpeni merkittävästi 1990-luvulla, kun Schottky-diodi integroitiin onnistuneesti CMOS-prosessiin.

Tässä väitöskirjassa on tutkittu radiotunnistusjärjestelmien radiotaajuisia komponentteja ja ilmiöitä UHF- ja millimetriaaltoalueella. Teoreettisen analyysin perusteella tehonsyöttö lukijalta tunnisteelle rajoittaa passiivisen UHF RFID -järjestelmän toimintaetäisyyden noin kymmeneen metriin. Lukijan vastaanottama signaali on tällä etäisyydellä heikko lähettimen kohinaan verrattuna. Tässä väitöskirjassa on esitetty kaksi mukautuvaa radioetuastetta lähettimen kohinan eristämiseksi vastaanottimesta.

Tunnisteantennin sivuunvirittyminen on yleinen ongelma radiotunnistuksessa. Antennin kiinnitysalustan johtavuus tai dielektrisyys muuttaa antennin resonanssitaajuutta, mikä voi estää tunnisteen havaitsemisen. Väitöskirjassa on kehitetty kaksi takaisinsirontaan perustuvaa antennimittausmenetelmää ilmiön tutkimiseksi. Lisäksi työssä esitellään antennirakenne, joka voidaan kiinnittää useille erityyppisille pinnoille antennin toiminnallisuuden heikentymättä.

Millimetriaaltoalueella radiotunnistuksessa voidaan käyttää erittäin laajaa tiedonsiirtokaistaa lyhyillä etäisyyksillä langattoman massamuistin nopeaan lukemiseen. Toisaalta pitkän kantaman sovelluksessa esimerkiksi autotutkia voitaisiin käyttää lukijalaitteina. Väitöskirjassa on tutkittu millimetriaaltojen käyttöä radiotunnistuksessa teoreettisesti sekä osoitettu tekniikan toimivuus kokeellisesti 60 GHz:n taajuudella.

# Preface

The work leading to this thesis has been carried out at the Centre of Sensors and Wireless Devices at VTT Technical Research Centre of Finland, Espoo, Finland, during 2003 – 2008. The thesis has been supported by The Finnish Foundation for Technology Promotion (TES), The Foundation of The Finnish Society of Electronics Engineers (EIS), and The Espoo Culture Foundation. The financial support is gratefully acknowledged.

I was introduced to RFID by my instructor, Dr. Timo Varpula. I thank Timo for the opportunity to work on the subject and for all the advice during the years. The work has been supervised by two professors, Kimmo Saarinen and Matti Kaivola. I wish to thank them both for their support. Professor Heikki Seppä deserves special thanks for the long discussions on RFID, universe and everything. Many problems in the prototypes were solved during these sessions with mind-blowing speed. I also thank the reviewers of the dissertation, Dr. Catherine Dehollain from EPFL of Switzerland and professor Lauri Sydänheimo from Tampere University of Technology for their time and effort on the quality of the thesis. I'm also keen to thank professor Pavel Nikitin from University of Washington, USA, for promising to act as the opponent in the defense.

I'm indebted to all the co-authors and colleagues. Especially Dr. Mervi Hirvonen, Dr. Tauno Vähä-Heikkilä, Dr. Nadine Pesonen and M.Sc. Kaarle Jaakkola, among others, have counseled me whenever needed. The advice of Dr. Kaj Nummila and all the other senior research staff has been invaluable. I want to thank all of my friends, especially those around the Round Table, whether at TKK or Gallows.

Sincere thanks for my parents Toini and Matti who have tiredlessly supported and encouraged me all my life. I wouldn't be here without You. I also want to thank my brother Antti for being there for me.

I thank Aino and and Ilmari for making daddy to think something else than his research, and reminding him of the joy of discovery. Finally, I thank my wife, Eeva, for everything: Like a night in the forest, like a walk in the rain...

Pekka Pursula, Espoo, December 2nd 2008.

# List of Publications

## Backscattering Communication and Applications

I P. Pursula, J. Marjonen, H. Ronkainen, and K. Jaakkola, "Wirelessly Powered Sensor Transponder for UHF RFID", *Transducers & Eurosensors'07 Conference*, Lyon, France, June 10 – 14, 2007, pp. 73 – 76.

II P. Pursula, T. Vähä-Heikkilä, A. Müller, D. Neculoiu, G. Konstantinidis, A. Oja, and J. Tuovinen, "Millimeter-Wave Identification – A New Short-Range Radio System for Low-Power High Data-Rate Applications", *IEEE Transactions on Microwave Theory and Techniques*, Vol. 56, Issue 10, pp. 2221 – 2228, October 2008.

## Transponder Antenna Design and Measurement

III M. Hirvonen, P. Pursula, K. Jaakkola, and K. Laukkanen, "Planar Inverted-F Antenna for Radio Frequency Identification", *IEE Electronics Letters*, Vol. 40, Issue 14 , pp. 848 – 849, July 2004.

IV P. Pursula, M. Hirvonen, K. Jaakkola, and T. Varpula, "Antenna Effective Aperture Measurement with Backscattering Modulation", *IEEE Transactions on Antennas and Propagation*, Vol. 55, No. 10, pp. 2836 – 2843, October 2007.

V P. Pursula, D. Sandström, and K. Jaakkola, "Backscattering-Based Measurement of Reactive Antenna Input Impedance", *IEEE Transactions on Antennas and Propagation*, Vol. 56, No. 2, pp. 469 – 474, February 2008.

## Adaptive RF Front End for Reader Device

VI P. Pursula, M. Kiviranta, and H. Seppä, "UHF RFID Reader with Reflected Power Canceller", accepted in *IEEE Microwave and Wireless Component Letters*, to be published in January 2009.

VII P. Pursula and H. Seppä, "Hybrid Transformer-Based Adaptive RF Front End for UHF RFID Mobile Phone Readers", *IEEE International Conference on RFID*, Las Vegas, USA, April 16 – 17, 2008, pp. 150 – 155.

# Author's Contribution

I The author is the responsible author of the paper. The author designed the air interface and the protocol of the system. He contributed to the RF front end design and is responsible for the RF -related measurements. The author wrote the paper except for Sections 1 and 3.2. He presented the paper as an oral contribution in the conference.

II The author is the responsible author of the paper. The author derived the equations of operation and gathered the other results and the review of components in Sections II and III. He participated in the measurements and analysed the measurement results. He wrote the paper except for Section IV.

III This is a collaborative paper. The author is responsible for the antenna measurements and the analysis of the measurement results together with M. Hirvonen. The author wrote the paragraph on the measurement method.

IV The author is the responsible author of the paper. The author derived the theory and analysed the measurement results and uncertainty. He is responsible for the wireless measurements together with M. Hirvonen. The author wrote the paper.

V The paper is based on an original idea by the author. He is responsible for the theoretical analysis, measurements and the analysis of the measurement results together with D. Sandström. The author wrote Sections I, V and VI.

VI The author is the responsible author of the paper. The author designed and developed the UHF reader prototype, and he was responsible for the measurements. The theoretical analysis is a collaborative work by all the authors. The author wrote Sections I, III and parts of IV.

VII The author is the responsible author of the paper. The author is responsible for all simulations, measurements and the analysis of the measurement results. The theoretical analysis is a collaborative work by all the authors. The author wrote Sections I, III, IV, V and parts of VI. He presented the paper as an oral contribution in the conference.

The papers are referred to throughout the thesis by their Roman numerals [I] – [VII].

# Contents

# 1 Introduction

Radio Frequency Identification (RFID) has gained lot of interest and publicity in the recent years. In particular in industries, where logistics are central to the business, RFID-based processes have been tested, piloted and implemented with enthusiasm verging on hype [1]. Radio frequency identification has promised to deliver unprecedented visibility of goods within the logistics chain, because the long read range enables automatic identification, which replaces manual work.

In addition to logistics, the applications of radio frequency identification seem almost endless [2]. Access control is the most typical application, since many companies use RFID-based key cards in their offices. Car immobilisers are based on RFID [3]. The technique is used for collecting road tolls [4], as well as for timing in mass sports events [5]. Cattle, pets, and a few people carry transponders for identification [6]. Systems that enable localisation of transponders have been used e.g. in hospitals for patient and personnel safety as well as for the control of the medical equipment inventory [7]. Recently, short range readers under the near-field communication (NFC) standard have been integrated to mobile phones [8]. At the same time, sensors are being implemented within RFID systems, which opens ever-more applications.

Sensor networks have been envisioned to be the next mega trend after the Internet. A major drawback, however, exists. The sensor nodes need power for operation, and batteries tend to run empty, even though the life time of a battery in a sensor node has been extended to ten years. Passive RFID provides an efficient solution to the problem: Powering the sensor node remotely from the reader eliminates the battery.

But what actually is the technology behind RFID? The system consists of a reader device and a number of transponders. The transponders are attached to the objects to be identified. They include a memory, where an identification code and possible additional information on the object are stored. The reader can access the memory of a nearby transponder, and read the information stored in the memory.

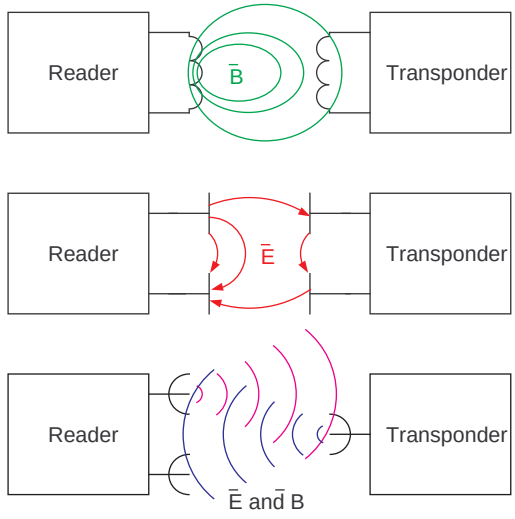


*Figure 1.1. Physical coupling between reader and transponder: Inductive coupling uses the magnetic field $\bar{B}$ of a coil (top). Capacitive coupling utilises the electric field $\bar{E}$ of a capacitor (centre). Electromagnetic coupling is based on wave propagation of both $\bar{E}$ and $\bar{B}$ (bottom).*

A variety of RFID systems exist. The systems differ in terms of range, size, cost and underlying technology and can be classified based on different characteristics, such as *coupling, operation frequency, transponder powering* and *implementation*.

The physical coupling between the reader and the transponder can be based on magnetic field (inductive coupling), electric field (capacitive coupling) or radiation field (electromagnetic coupling). These coupling methods are illustrated in Fig. 1.1. The inductive and capacitive couplings utilise the near-fields of a coupling element, i.e. a coil and a capacitor, respectively. The nature of the near-fields limits the read range approximately to the size of the coupling element. The electromagnetic coupling is based on electromagnetic waves, which are generated by an antenna, and which propagate far from the antenna.

The operation frequency of near-field systems varies from low to high frequencies, i.e, from 100 kHz to 13.56 MHz. The 13.56 MHz band is globally reserved for inductive RFID. Electromagnetically coupled systems operate at higher frequencies, usually from 400 MHz to 5 GHz, even though research takes place also in the millimetre waves, up to 60 and 77 GHz. Most of the electromagnetically coupled systems operate at ultra high frequencies (UHF), i.e. around 900 MHz.

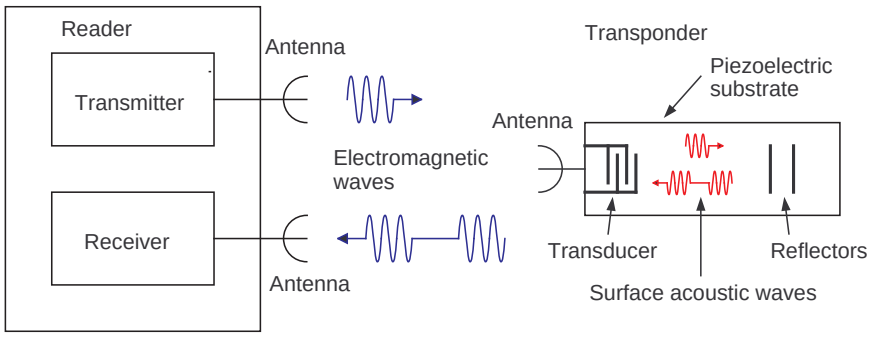


*Figure 1.2. The operation principle of SAW RFID. The reader sends a short pulse of electromagnetic (EM) waves, which are transformed to surface acoustic waves (SAW) in the transponder. The waves are reflected with different time delays and transformed back to EM waves for transmission to the reader.*

A passive transponder is powered up by the reader transmission. A semi-passive transponder has a battery, but relies on backscattering modulation for uplink (transponder to reader) communication. This enables a longer range than with a passive transponder, while providing a long battery lifetime. Active transponders generate also the carrier for uplink communications from the power of the battery.

The transponder memory can be implemented with microelectronics on silicon or with printing technology on an organic or an inorganic substrate. Also surface acoustic wave (SAW) propagation on a piezoelectric material can be used. The integrated circuits (IC) on silicon include a state machine that runs a program much like a microprocessor. The transponders based on printed organic or inorganic transistors have the same operational principle. In SAW RFID, the slow propagation of surface acoustic waves is utilised to create reflections of the reader transmission with different time delays (Fig. 1.2).

Most of the recent interest in RFID has been concentrated on silicon-based passive electromagnetically coupled systems at UHF. These systems deliver more than 5 metres of reliable read range with transponders that cost less than 10 Euro cents. The other systems can be superior in other aspects. For example, inductive systems can deliver much better security and encryption features [2], and SAW-based systems deliver a longer range [9].

Printed electronics might provide another low-cost implementation of the transponders in the future. The transponder antenna for HF and UHF RFID can be printed with ink that includes metallic nanoparticles (see

e.g. [10]). The transistors for the transponder electronics can be printed with inorganic or organic semiconductor ink. A mobility of 0.1 $cm^2/Vs$ is achieved in organic transistors [11]. Inorganic semiconductors have been used in printed electronics to fabricate higher quality transistors with mobilities of 80 $cm^2/Vs$ [12], but they are still slower and lossier than the transistors on silicon, where the bulk electron mobility is 1500 $cm^2/Vs$. Functional systems have been implemented for frequencies up to 13.56 MHz, both organic [13] and inorganic [12], but often the protocols of the systems are simplified (see e.g. [14]), and they do not comply with the standards.

This Thesis studies passive electromagnetically coupled RFID systems at UHF and millimetre waves. The study concentrates on silicon-based systems, even though some of the analysis is independent of the transponder implementation. This choice reflects the author's opinion of the most feasible RFID system configuration. The ultra high frequency provides a good compromise between size and read range, and the maturity of the silicon technology makes it the best choice both technically and economically, at least for many years to come.

The author has been involved in proposing RFID at millimetre waves, a technique called Millimetre Wave Identification (MMID). Millimetre waves span up in frequency from 30 GHz, where the wavelength of the radiation is below 1 cm. The advantages of millimetre waves include high data rates, small directional antennas, and the possibility to use automotive radars as reader devices. MMID is technically feasible today, even though the components are expensive. But the technology is becoming economically more attractive with CMOS-processes scaling up to 60 GHz and beyond.

The operational principle of passive UHF RFID is summarised in Fig. 1.3. The reader transmits a modulated carrier signal. The transponder rectifies the carrier to power itself up. Downlink communication, i.e. from reader to transponder, includes amplitude modulated commands. The uplink communication (from transponder to reader) is realised with backscattering modulation. The reader sends a carrier signal when the transponder responds. The transponder IC modulates its input impedance, which leads to a modulation of the signal scattered by the transponder. Both amplitude and phase modulation can be utilised. The signal transfer from the transponder to the reader is based on reflection, like in the optical bar code systems. But in RFID, at radio frequencies, a coherent detection of the reflection can be used, which makes the detection more sensitive. This is emphasised in Fig. 1.3 by drawing the common local oscillator for the transmitter and the receiver.

The understanding of antenna scattering and its detection is crucial to

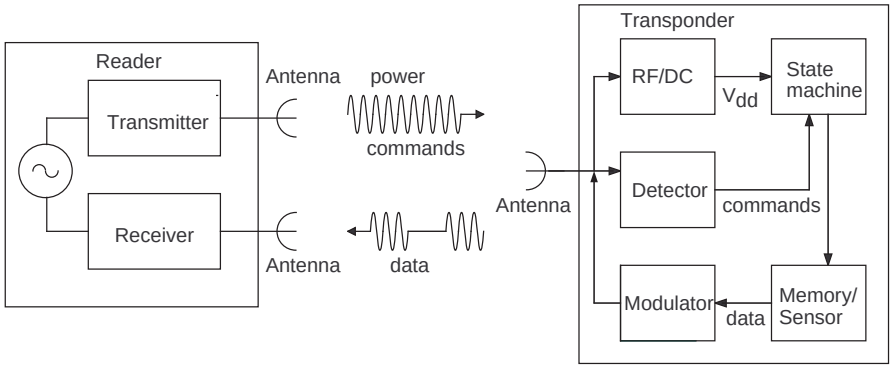


*Figure 1.3. Components of a passive UHF RFID system. A reader with coherent detection (left) and a transponder with an antenna connected to a silicon-based integrated circuit (right).*

the reliability of an RFID system. This Thesis studies the radio frequency (RF) components, i.e. the transponder antenna and reader front end, and the antenna scattering. In the next chapter, the fundamental theory for transponder powering and communication by backscattering modulation is derived. The analysis is applied to UHF, where an RFID chip for sensor applications is also presented [I]. The RFID concept is extended to millimetre waves theoretically and experimentally [II].

In Chapter 3, the transponder antenna and its scattering are further discussed. A platform-tolerant transponder antenna structure is presented [III]. The scattering of transponders is measured, and two scattering-based measurement techniques for transponder antenna characterisation are introduced [IV, V]. Last, but not least, the RFID reader device is studied in Chapter 4. The development of two RFID readers with adaptive RF front ends is presented [VI, VII].

## 1.1 History

Electromagnetic coupling is based on electromagnetic wave propagation, which was first predicted by Maxwell, when he derived the electromagnetic wave equations in 1864 [15]. Hertz was the first to experimentally generate and detect electromagnetic waves beginning in 1888. The development of the radio technology culminated in Marconi making his famous transmission of data over the Atlantic Ocean in 1901. Tesla was experimenting

with the wireless radio at the same time, but is known better for his experiments on wireless power transfer. He had several patents relating to power transfer. Even though Tesla imagined using wireless power transfer over considerable distances, the power transfer systems described by him are basically near-field systems, consisting of two coupled resonant circuits [16]. For global wireless power transfer he suggested using the earth as a resonator [17]. In 1900, in one of his patents [16], Tesla rejects the use of electromagnetic waves for power transfer:

"It is to be noted that the phenomenon here involved in the transmission of electrical energy is one of true conduction and is not to be confounded with the phenomena of electrical radiation which have heretofore been observed and which from the very nature and mode of propagation would render practically impossible the transmission of any appreciable amount of energy to such distances as are of practical importance."

It took half a century before radio wave power transmission was developed further. Friis derived the transmission equation in 1946 [18]. High microwave power transfer has been developed since the 1950s, and a power of 30 kW was transferred over a distance of 1 mile in 1975 [19]. Nowadays, radio waves are used in the passive electromagnetically coupled RFID systems for wireless power transfer of micro- and milliwatts over distances of up to 10 m.

In 1948, Stockman proposed using modulated backscattering for communication [20]. He used corner reflectors and modulated the backscattering by moving one of the metal plates of the reflector. For example, by modulating the reflector plate by voice he succeeded in transferring the signal over a hundred yards.

King was one of the first to measure and interpret antenna scattering as a function of antenna load [21] in 1949. The theory was developed further by Harrington, who derived the scattering equation for loaded scatterers using a linear three-port network in 1964 [22]. Since then the research field has diversified and load modulation has been used for example in electric field measurements [23], as well as the measurement of antenna gain [24], antenna input impedance [25], and antenna scattering matrix [26]. The author has studied backscattering-based measurement techniques in the case of RFID in [IV, V]. Today's RFID technology relies on backscattering modulation for uplink communication.

The history of RFID cannot be written without mentioning the passive microphone developed by Theremin. The microphone was placed within the Great Seal of Unites States and presented to the US Ambassador in Berlin by the Russians in 1946. The microphone was used for spying for

six years, before it was found by the Americans in 1952. The device was completely passive, including only an antenna and a cavity resonator with a moving diaphragm [27].

During World War II, the Royal Air Force used an RFID based system to identify friendly aeroplanes. The Interrogate-Friend-or-Foe (IFF) system was similar to the transponders that commercial aeroplanes carry nowadays. The transponders are active, and usually use UHF frequencies at around 1 GHz [28].

The inductive RFID systems have been widely adopted for access control since the 1990s. In the beginning of the 2000s, they were standardised under the Near-Field Communication (NFC) Forum, which has lead to readers embedded in mobile phones (see e.g. [8]).

A passive UHF RFID system was first demonstrated in 1975 by Koelle, Depp and Freyman [29]. Commercial systems began to emerge in the 1980s, but the development of Schottky diodes on a CMOS circuit in the 1990s can be considered a breakthrough [30]. This advance allowed long-range and low-cost transponders, see e.g. [31, 32]. At this time, also standardisation under the International Organization for Standardization (ISO) and the Auto-ID Center (now EPCglobal) began.

## 1.2 Regulations and Standards

To ensure the successful coexistence of the myriads of radio devices of our daily lives, the electromagnetic spectrum is divided into separate bands for different radio applications. Unfortunately, a global band for the UHF RFID does not exist, but the allocated bands vary from region to region. The frequency bands and allowed transmission (TX) power for a number of regions are summarised in Table 1.1. The transmission power is expressed as equivalent isotropic radiated power (eirp), i.e., $P_{eirp} = G_{tx}P_{tx}$, where $G_{tx}$ is the transmitter antenna gain and $P_{tx}$ the power fed to the antenna. The equivalent radiated power (erp) is similarly defined, but uses antenna gain over dipole (dBd). The two are related as $P_{eirp} = 1.64P_{erp}$.

In addition to the radio regulations, the physical layer of RFID systems, including modulation, encoding etc., is standardised by the International Standardisation Organisation and EPCglobal. These have issued the UHF RFID air interface standards ISO 18000-6 [33] and EPC Gen2 [34], respectively. The standards are identical, except for a few application identifier bits in the transponder memory mapping. These standards have become

*Table 1.1. Radio regulations on UHF RFID in different regions.*

| Region | Frequency (MHz) | TX Power (maximum) | Regulation | Ref |
|---|---|---|---|---|
| Europe | 869.4 – 869.65 | 0.5 $W_{erp}$ | EN 300 220 | [35] |
| Europe | 865 – 868 | 2.0 $W_{erp}$ | EN 302 208 | [35] |
| USA | 902 – 928 | 4.0 $W_{eirp}$ | FCC Part 15 | [36] |
| Korea | 908.5 – 914 | 4.0 $W_{eirp}$ | | |
| Japan | 952 – 954 | 4.0 $W_{eirp}$ | | |
| China | 840.25 – 844.75 | 2.0 $W_{erp}$ | | [37] |
| China | 920.25 – 924.75 | 2.0 $W_{erp}$ | | [37] |

the most utilised in the field in recent years.

The physical layers of some air-interface standards and protocols are presented in Table 1.2. The study presented in this thesis can be utilised for any modulation and coding scheme, and the air interface standards are not discussed further. The allocated frequency and the allowed power define the fundamental limits of the RFID system read range, as will be seen in the next chapter.

*Table 1.2. Physical layers of some air-interface standards and protocols for UHF RFID.*

| Standard/ Protocol | Downlink | | Uplink | | Ref |
|---|---|---|---|---|---|
| | Modulation | Encoding | Modulation | Encoding | |
| ISO 18000-6A | ASK | PIE | ASK | FM0 | [33] |
| ISO 18000-6B | ASK | Man-chester | ASK | FM0 | [33] |
| ISO 18000-6C | (PR-) ASK | PIE | ASK PSK | FM0 MMS | [33] |
| EPC Gen2 | (PR-) ASK | PIE | ASK PSK | FM0 MMS | [34] |
| Tagidu | PR-ASK | PIE | PSK | FM0 NRZ 3Phase1 | [32] |

PIE = pulse interval encoding
(PR-)ASK = (phase reversal) amplitude shift keying
PSK = phase shift keying
MMS = Miller-modulated subcarrier
NRZ = non-return to zero

# 2 Communication by Backscattering Modulation

A passive RFID system has two principal constraints limiting its operation: the power transfer to the transponder and the power received by the reader. The electromagnetic wave propagation phenomena are crucial to the success of RFID, and have been widely studied. One of the first analyses of the RFID read zone was presented by Rao et al. [38]. The power transfer to a transponder was analysed as a function of antenna load by Karthaus and Fischer [39]. Nikitin and Rao [40, 41] included a number of unidealities in the discussion, e.g. multipath propagation and polarisation. Recently, Fuschini et al. [42] have analysed the transponder antenna scattering further. The author has studied the phenomena in [II, IV].

The two-way power budget of an RFID system is presented in Fig. 2.1. The figure describes a passive UHF RFID with a transponder near its maximum operational range. The system has two critical power levels,

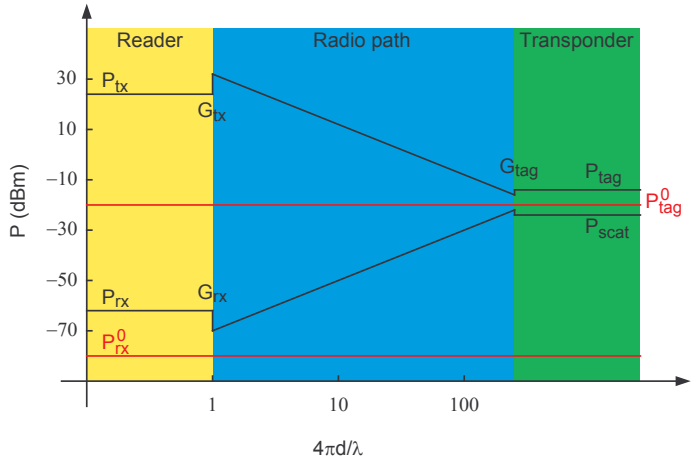


*Figure 2.1. Power budget diagram of an RFID system.*

the transponder sensitivity $P^0_{tag}$ and the reader sensitivity $P^0_{rx}$, i.e. the minimum power levels required by the transponder and the reader.

Figure 2.1 shows the symmetry of the up- and downlinks in an RFID system. The radio path is equal in both directions. The effect of the antenna gain is shown as steps in the power level. The transponder uses some of the incident power for powering up the integrated circuit (IC) and some for backscattering modulation. The modulation loss determines the difference of the power $P_{tag}$ transferred to the IC and the scattered power $P_{scat}$. The power budget of an RFID system is comprehensively discussed in the next sections.

## 2.1 Effective Aperture and Radar Cross Section

The power transfer to the transponder and the power scattered by the transponder are described in terms of the effective aperture $A_e$ and the radar cross section $\sigma$ of the transponder antenna, respectively. To derive equations for the effective aperture and the radar cross section, the transponder is modelled as a series circuit shown in Fig. 2.2. The circuit consists of series resistances and reactances of an antenna (subscript $A$) and a load (subscript $L$), and a voltage source with amplitude $V$ describing the incident radiation field.

The effective aperture $A_e$ and the radar cross section $\sigma$ can be expressed in terms of the power dissipated in the load and antenna resistances, respectively [43]

$$\begin{aligned} A_e &= \frac{\frac{1}{2}R_L|I|^2}{S}, \\ \sigma &= \frac{\frac{1}{2}G_A R_A|I|^2}{S}. \end{aligned} \tag{2.1}$$

Here $I$ is the complex amplitude of the current in the circuit. The antenna gain $G_A$ in the radar cross section equation takes into account the antenna losses and directivity when the scattered power is re-radiated. The power is normalised to the incident field power intensity $S$, which is related to the voltage $V$. In a conjugate match, the power dissipated in the load and antenna resistances are equal, and they can be identified with the available power in the Friis equation [18]

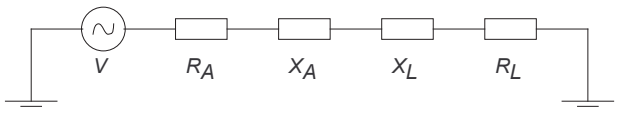


*Figure 2.2. The series model of a loaded antenna.*

$$\frac{V^2}{8R_A} = \frac{G_A\lambda^2}{4\pi}S. \tag{2.2}$$

Combining Eqs. (2.1) and (2.2), the effective aperture and the radar cross section can be written as [IV]

$$\begin{aligned} A_e &= \frac{G_A\lambda^2}{4\pi}\frac{4R_AR_L}{(R_A+R_L)^2+(X_A+X_L)^2}, \\ \sigma &= \frac{G_A^2\lambda^2}{4\pi}\frac{4R_A^2}{(R_A+R_L)^2+(X_A+X_L)^2}. \end{aligned} \tag{2.3}$$

The equations consist of a maximum aperture term multiplied by a mismatch term. The mismatch term can be expressed with the aid of a reflection coefficient, known as the Kurokawa power reflection coefficient [44, 45]

$$\Gamma = \frac{Z_L - Z_A^*}{Z_L + Z_A}. \tag{2.4}$$

The current in the circuit can now be written as

$$I = \frac{V}{Z_A + Z_L} = \frac{V}{2R_A}\left(1-\Gamma\right). \tag{2.5}$$

The power dissipated in the load has two expressions in terms of the reflection coefficient,

$$\begin{aligned} P_L &= \frac{1}{2}R_L|I|^2 \\ &= \frac{V^2R_L}{8R_A^2}\left|1-\Gamma\right|^2 \\ &= \frac{V^2}{8R_A}\frac{4R_LR_A}{|Z_L+Z_A|^2} \\ &= \frac{V^2}{8R_A}\left(1-|\Gamma|^2\right). \end{aligned} \tag{2.6}$$

The expression on line 2 of Eq. (2.6) follows directly from Eq. (2.1). The expression on line 4 can be considered as the product of the incident power and the power transmission coefficient. Now the equations for the effective aperture and radar cross section can then be written as [II]

$$\begin{aligned} A_e &= \frac{G_A \lambda^2}{4\pi} \left(1 - |\Gamma|^2\right), \\ \sigma &= \frac{G_A^2 \lambda^2}{4\pi} |1 - \Gamma|^2 . \end{aligned} \tag{2.7}$$

The mismatch terms now look more familiar.

In a conjugate match, i.e. for $\Gamma = 0$, the expressions in Eq. (2.7) reduce to the well-known aperture equations presented already by Friis [18] and Harrington [22]

$$\begin{aligned} A_e &= \frac{G_A \lambda^2}{4\pi} \\ \sigma &= \frac{G_A^2 \lambda^2}{4\pi} = G_A A_e. \end{aligned} \tag{2.8}$$

## 2.2 Effect of Modulation

To achieve actual data transfer in the uplink, a modulation between two load impedance states $Z_1$ and $Z_2$, or reflection coefficients $\Gamma_1$ and $\Gamma_2$, is required. Assuming an FM0 coding scheme, which is used in the EPC Gen2 RFID standard [34], a square wave can be taken as the modulation waveform. Explicitly, the modulation has the form

$$\Gamma(t) = \begin{cases} \Gamma_1 & , \quad \frac{2\pi}{\omega_m}\left(k - \frac{1}{2}\right) < t < \frac{2\pi k}{\omega_m} \\ \Gamma_2 & , \quad \frac{2\pi k}{\omega_m} < t < \frac{2\pi}{\omega_m}\left(k + \frac{1}{2}\right) \end{cases}, \tag{2.9}$$

where $\omega_m$ is the modulation frequency, and $k$ is an integer. The effect of the duty cycle of the modulation waveform is further explored in [46].

The power available to the transponder is the average of the powers in each individual load state. Thus the effective aperture becomes [II]

$$A_e^m = \frac{G_A \lambda^2}{4\pi} \left(1 - \frac{1}{2}\left[|\Gamma_1|^2 + |\Gamma_2|^2\right]\right), \tag{2.10}$$

where the superscript $m$ is added to denote the modulated case.

The current $I$ in the circuit includes contributions at all the harmonics of the modulation frequency. Hence also the radar cross section has components on all the frequencies. The zeroth harmonic, i.e. the DC component, describes the scattering at the carrier frequency, and the other harmonic contributions of the modulation frequency form a comb of sidebands around the carrier.

In [IV], the radar cross section component $\sigma_1$ at the fundamental modulation frequency is calculated using Fourier expansion of the modulated current. In [II], the radar cross section $\sigma_0$ at the carrier frequency and the radar cross section $\sigma_m$, which describes the scattered power at all the harmonics of the modulation frequency, are presented. The Fourier expansion is now elaborated here to link these radar cross section terms together.

The Fourier series of the current is calculated in [IV], but not expressed with the reflection coefficient. However, the Fourier series of a square wave is well known, and can be expressed in terms of the reflection coefficient

$$\begin{aligned} I &= \frac{1}{2}I_0 + \sum_{k=1,3,5,\ldots} I_k \sin(k\omega_m t) \ \text{, where} \\ I_0 &= \frac{V}{2R_A}[2 - (\Gamma_1 + \Gamma_2)], \\ I_k &= \frac{V}{2R_A}\frac{2}{k\pi}(\Gamma_1 - \Gamma_2). \end{aligned} \tag{2.11}$$

The scattered power of each of the frequency components can be calculated by squaring the corresponding Fourier component of the frequency. The radar cross section components become

$$\begin{aligned} \sigma_0 &= \frac{G_A^2\lambda^2}{4\pi}\left|1 - \frac{1}{2}(\Gamma_1 + \Gamma_2)\right|^2, \\ \sigma_k &= \frac{G_A^2\lambda^2}{4\pi}\frac{2}{k^2\pi^2}|\Gamma_1 - \Gamma_2|^2. \end{aligned} \tag{2.12}$$

In [IV], a square modulation of the load reactance was studied. The load impedances $Z_1 = Z_A^* + j\Delta X$ and $Z_2 = Z_A^* - j\Delta X$ are used. Equations (11) and (14) in [IV] give the effective aperture $A_e^m$ and the radar cross section $\sigma_1$. The effective aperture is an average of the apertures of the individual impedance states, as suggested by Eq. (2.10). Using Eq. (2.12) for the case of the reactive modulation, the radar cross section $\sigma_1$ becomes

$$\sigma_1 = \frac{\lambda^2 G_A^2}{4\pi} \frac{16}{\pi^2} \frac{R_A^2 \Delta X^2}{(R^2 - X^2 + \Delta X^2)^2 + 4R^2 X^2}, \tag{2.13}$$

which is the equation given by the analysis in [IV] (see also Errata).

The radar cross section $\sigma_m$ associated with the overall scattered power can be calculated from the sum of the terms $\sigma_k$, i.e. $\sigma_m = \Sigma_k \sigma_k$ . Using the definition of the Riemann Zeta Function $\zeta(x)$ [47],

$$\zeta(2) = \sum_{k=1,2,3,\ldots} \frac{1}{k^2} = \frac{\pi^2}{6}, \tag{2.14}$$

the sum included in the radar cross section can be calculated as

$$\sum_{k=1,3,5,\ldots} \frac{1}{k^2} = \sum_{k=1,2,3,\ldots} \frac{1}{k^2} - \frac{1}{4} \sum_{k=1,2,3,\ldots} \frac{1}{k^2} = \frac{\pi^2}{8}.$$

Hence, the modulated radar cross section becomes [II]

$$\sigma_m = \frac{G_A^2 \lambda^2}{16\pi} |\Gamma_1 - \Gamma_2|^2 = \frac{G_A^2 \lambda^2}{4\pi} m. \tag{2.15}$$

This is the radar cross section that describes the information carrying scattering. Here, $m = \frac{1}{4} |\Gamma_1 - \Gamma_2|^2$ is the modulation index or modulation loss. It can have values $0 \leq m \leq 1$.

The result for $\sigma_0$ in Eq. (2.12) and $\sigma_m$ in Eq. (2.15) can also be derived by arranging the modulated current to even and odd terms

$$I = \frac{V}{2R_A} \left[ 1 - \frac{1}{2} (\Gamma_1 + \Gamma_2) + \frac{1}{2} (\Gamma_1 - \Gamma_2) \Theta(t) \right], \tag{2.16}$$

where $\Theta(t)$ is a square wave with unity amplitude

$$\Theta(t) = \begin{cases} -1 & , \quad \frac{2\pi}{\omega_m} \left(k - \frac{1}{2}\right) < t < \frac{2\pi k}{\omega_m} \\ 1 & , \quad \frac{2\pi k}{\omega_m} < t < \frac{2\pi}{\omega_m} \left(k + \frac{1}{2}\right) \end{cases}. \tag{2.17}$$

The radar cross section terms $\sigma_0$ and $\sigma_m$ follow directly, if the odd and even currents are inserted to Eq. (2.1). However, this analysis does not provide an expression for the terms $\sigma_k$ for $k = 1, 2, 3, ...$ associated with the harmonics of the modulation frequency. The Fourier analysis provided also the term $\sigma_1$, and enabled comparing the expressions and analyses in [II] and [IV].

The analysis presented above did not make any assumptions concerning the type of the load modulation. The reflection coefficient suffices to describe the modulation in terms of the transferred and scattered power. In general, the transponder modulates both the amplitude and the phase of the scattered signal. The analysis gives the scattered power, independent of the type of modulation.

Usually, mainly either load resistance or reactance is modulated. Amplitude and phase modulation can arise from both types of load modulation. For example, modulation of the load resistance with states $Z_1 = 0 - jX_A$ and $Z_2 = R_A/2 - jX_A$ gives the reflection coefficients $\Gamma_1 = 1$ and $\Gamma_2 = 1/3$. Because the reflection coefficients have the same phase, but unequal magnitude, amplitude modulation arises. On the other hand, states $Z_1 = 0 - jX_A$ and $Z_2 = \infty - jX_A$ lead to reflection coefficients $\Gamma_1 = 1$ and $\Gamma_2 = -1$. They are equal in magnitude but opposite in phase. Hence phase modulation arises. In a similar manner, reactive load modulation can give rise to both amplitude and phase modulation.

Because of its simplicity, a switched capacitor or a switched resistor modulator is often used. Hence the scattered signal will include both phase and amplitude modulation. The reader needs quadrature downmixers to detect both amplitude and phase modulation and advanced algorithms are required for optimal detection.

## 2.3 Power Transfer and Received Power

Using the effective aperture from Eq. (2.10), the power $P_{tag}$ transferred to the transponder can be calculated from the Friis equation

$$P_{tag} = A_e^m \frac{G_{tx} P_{tx}}{4\pi d^2}, \tag{2.18}$$

where the subscript $tx$ stands for the reader transmitter and $d$ is the distance between the transponder and the reader. The transferred power must be higher than the transponder sensitivity $P_{tag}^0$, which depends greatly on the properties of the transponder. The sensitivity $P_{tag}^0$ describes the minimum RF power that must be transferred to the integrated circuit (IC) of the transponder.

Often the unmodulated aperture $A_e$ in Eq. (2.7) is used in the Friis equation instead of the average aperture $A_e^m$ of Eq. (2.10). There are many reasons for this. First, the impedances of both of the IC modulation states are not always known. Usually only one impedance state is given in publi-

cations. Further, the modulation index is often quite low, less than -6 dB. Hence the error due to the simpler expression is small. The IC properties are further discussed in Section 2.4.

The power $P_{rx}$ received by the reader is given by the radar equation using the modulated radar cross section from Eq. (2.15)

$$P_{rx} = \sigma_m \frac{\lambda^2 G_{tx} P_{tx} G_{rx}}{(4\pi)^3 d^4}, \tag{2.19}$$

where the subscript $rx$ stands for the reader receiver (see Errata). The received power must be greater than the reader sensitivity $P^0_{rx}$, which is limited by the noise seen by the receiver. This will be further discussed in Section 2.5 and Chapter 4.

Which one of Eqs. (2.18) and (2.19) imposes the more stringent limit for the range of the RFID system? It depends on many parameters of the system: the antenna gains, distance, and especially on the transponder and reader sensitivities. An overview of state-of-the-art transponder ICs and readers needs to be presented to determine proper values of the sensitivities $P^0_{tag}$ and $P^0_{rx}$.

## 2.4 Transponder Sensitivity

The sensitivity of a passive transponder IC depends mainly on the transponder DC power consumption and rectifier efficiency $\eta$. The efficiency is usually only 10 – 40 %, because of RF power leaks to substrate through paracitic elements and because the incident voltages are low compared with the threshold voltage and thermal noise of the rectifying element. The parasitic leakage can be diminished by using a narrow-line-width process and a high-resistivity substrate. The DC power consumption depends on the circuit functionality. Memory access consumes less power than sensor interfacing, for example.

In [I], a sensor RFID IC is presented. The block diagram and chip photograph of the sensor chip are presented in Fig. 2.3. The IC has a 10 bit analog-to-digital converter (ADC) for an external sensor. The IC includes all RF and baseband analog and digital electronics that are needed for the wireless readout of the external sensor.

Table 2.1 presents an overview of the passive UHF RFID ICs published in the literature. The sensitivity is often expressed in terms of a DC current consumption from a certain voltage. Whenever possible, the sensitivity has been transformed to the RF power incident to the IC, which is referred

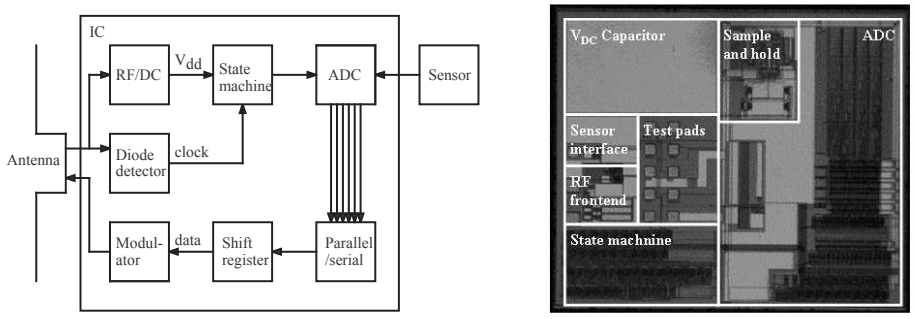


*Figure 2.3. The block diagram (left) and photograph (right) of the wireless sensor IC [I].*

to as $P^0_{tag}$. The modulation index $m$, which is needed to calculate the radar cross section $\sigma_m$, depends on the modulator design. Common designs include a capacitance diode, a switched capacitor and a switched resistor. Unfortunately the modulation index $m$ and the rectifier efficiency $\eta$ are presented in only a few publications.

In addition to the passive UHF chips, Table 2.1 includes a SAW-based sensor chip [48], one inductive sensor system on package [49], and one semi-passive memory IC [50]. The transponder sensitivity varies at least by a factor of 1000, depending on the chip functionality. Roughly, the chips can be divided into two classes: memory ICs and sensor ICs.

The memory ICs have a sensitivity of the order of 1 – 10 $\mu W_{RF}$. The ICs with the sensors or sensor interfaces require more power, from 100 $\mu W_{RF}$ to 10 $mW_{RF}$. This is not surprising, as high precision and power consumption are contradictory optimisation parameters in ADCs, which can be understood to be a consequence of the thermal noise in resistors: the greater the resistor, the less power is dissipated, but the higher is the noise generated. Unfortunately the RF sensitivity of the sensor IC in [51] is not provided, but assuming a typical rectifier efficiency of $\eta = 20$ %, the sensitivity would be about 25 $\mu W_{RF}$.

The 10 bit ADC sensor readout presented in [I] stands up well in the comparison. The power consumption of the IC is only 30 $\mu W_{DC}$. All the other sensor ICs in Table 2.1 have much higher power consumption, except for [51]. To date, the chip presented in [I] seems to be the only published UHF RFID IC with an ADC for external sensors. However, sensor ICs for RFID are commercially interesting, and a lot of unpublished development is probably carried out by the industry.

*Table 2.1. Review of RFID Integrated circuits.*

| $f_0$ (MHz) | $Z_L$ ($\Omega$) | $m$ (dB) | Sensitivity ($\mu W_{RF}$) | Sensitivity ($\mu W_{DC}$) | $\eta$ (%) | Process | Features | Ref | Year |
|---|---|---|---|---|---|---|---|---|---|
| 915 | — | — | — | — | — | SAW | analog uplink, temp sensor | [48] | 1987 |
| 865 | 6-$j$210 | -6 | 16.7 | 3.0 | 18 | 0.5 $\mu$m CMOS +Schottky | | [39] | 2003 |
| 860 – 960 | — | — | — | 5.1 | — | 0.25 $\mu$m CMOS | 10 bit? ADC, internal temp and photo sensor | [51] | 2005 |
| 3 | — | — | — | 341 | — | 3 $\mu$m BiCMOS | inductive, analog uplink, external sensors for temp, pressure, RH% | [49] | 2005 |
| 2 450 | 5-$j$130 | <-6 | 2.7 | 1.0 | 37 | 0.5 $\mu$m Si on Sapphire | | [52] | 2005 |
| 450 & 900 | 12-$j$10 | — | — | 4 000 | — | 0.25 $\mu$m CMOS | 5 bit ADC, uplink 7 Mbit/s up-/downlink 900/450 MHz | [53] | 2006 |
| 915 | — | — | 400 – 1 000 | — | — | not integrated | 10 bit ADC, EPC Gen1 | [54] | 2007 |
| 869 | 22-$j$145 | -12 | 4 300 (250) | 30 (30) | 0.7 (12) | 1.5 $\mu$m BiCMOS (+Schottky) | 10 bit ADC | [I] | 2007 |
| 953 | — | — | 80 | 29 | 36 | 0.35 $\mu$m CMOS | | [55] | 2007 |
| 2 450 | 92-$j$867 | — | 12.5 | — | — | 1 $\mu$m CMOS +Schottky | ISO-18000-4B, semi-passive | [50] | 2007 |
| 860 – 960 | 27-$j$200 | — | 15.8 | — | — | CMOS | EPC Gen2 | [56] | 2008 |

## 2.5 Reader Sensitivity

Table 2.2 presents a review of the receiver parameters of published and commercialised RFID readers. The most important parameters are the reader sensitivity and the input compression point $P_{1dB}$. The sensitivity describes the lowest received signal power that can be differentiated from noise. The input compression describes the highest incident power that the receiver tolerates. In general, the higher the input compression point, the worse the sensitivity. The sensitivity and input compression will be discussed further in Chapter 4.

The sensitivity is limited by the noise in the receiver. This includes the thermal noise of the receiver itself, but also the transmitter noise has an impact: Because the receiver and the transmitter are operating simultaneously at the same frequency, the transmitter signal easily couples to the receiver. Hence, the sensitivity is a function of the incident carrier power, or the TX–RX coupling. The reader ICs [57, 58] have two operating modes: The best sensitivity is achieved with the lowest $P_{1dB}$ and vice versa.

The ICs and commercialised readers have a sensitivity of -96 – -70 dBm at a reliable communication level defined by a reasonably low bit error rate (BER) or packet error rate (PER) and a different incident carrier power. In [VI] a sensitivity of even -100 dB is achieved with unity signal-to-noise ratio (SNR). In practice, at least an SNR = 10 dB is required for reliable communication (approximately BER $< 10^{-3}$ [46, 58]). The bandwidths of the readers are similar, even though they are presented differently. Hence, the reader presented in [VI] has a similar sensitivity to the commercial readers, but a higher compression point. However, the sensitivity in [VI] is still 20 dB over the thermal noise limit. The reader dynamic range will be further discussed in Chapter 4.

## 2.6 Read Range of UHF RFID

After reviewing the transponders and the readers, it is now possible to choose some typical values for transponder and reader sensitivity to analyse the system. For a graphical analysis of the read range, typical UHF RFID system parameters are chosen. The transponder sensitivity $P^0_{tag} = 10\mu$W is 2 dB better than the EPC Gen2 chip in [56]. The reader sensitivity $P^0_{rx} = -100$ dBm is the best value in the reader review presented in Table 2.2.

*Table 2.2. Review of Readers.*

| Sensitivity (dBm/Hz) | Sensitivity (dBm) | $\Delta f$ | $P_{1dB}$ (dBm) | Process | Features | Ref | Year |
|---|---|---|---|---|---|---|---|
| — | — | — | — | — | ISO 18000-6C | [59] | 2007 |
| — | -96 – -80 (BER 0.1 %) | 40 kbit/s | — | not integrated | ISO 18000-6C | [60] | 2007 |
| — | -96 – -83 (PER 1 %) | 40 kbit/s | 4 – 11 | 0.18 $\mu$m SiGe BiCMOS | ISO 18000-6C | [57] | 2007 |
| — | -80 – -70 (BER 0.001 %) | 40 kbit/s | -10 – 8 | 0.18 $\mu$m CMOS | ISO 18000-6 | [58] | 2008 |
| -155 – 140 | -100 – -85 (SNR 1) | 200 kHz | 15 | not integrated | | [VI] | 2008 |

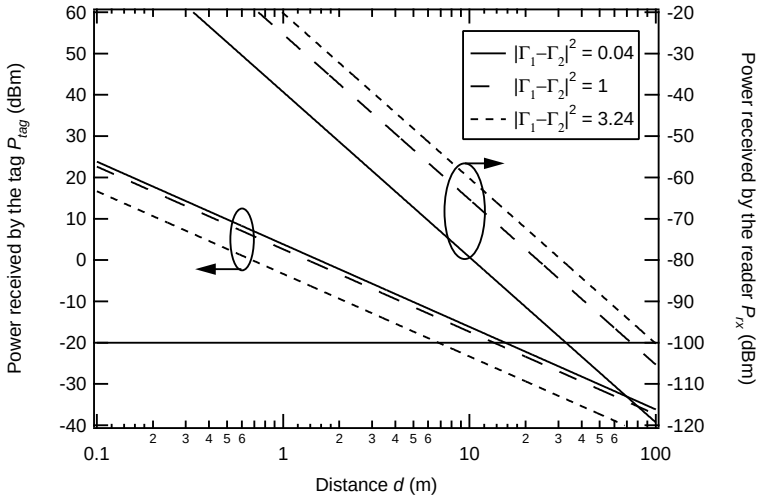


*Figure 2.4. The limiting factors on the UHF RFID range at 867 MHz with $G_{tx}P_{tx}$ = 2 $W_{erp}$, $G_{rx}$ = 8 dBi, $G_A$ = 0 dBi [II].*

The link budget of the RFID system is summarised in Fig. 2.4 (see Errata). Both the transferred and received powers are presented as a function of the operational distance at 867 MHz with several modulation index values. Ideal modulation is assumed, i.e. $\Gamma_1 = -\Gamma_2$. The power scales have been set in such a way that the horizontal line represents both $P^0_{tag}$ and $P^0_{rx}$.

Naturally, the more power is scattered, the less power is transferred to the transponder. The choice of the modulation index depends greatly on the system variables. If the range is limited by the power transfer, the modulation should be as shallow as possible ($m \approx 0$), and vice versa: If the scattered power is the limiting factor, the modulation should be as deep as possible ($m \approx 1$).

According to Fig. 2.4, the read range of a typical passive RFID system at UHF is power transfer limited to a range of 10 m. However at $d = 10$ m, the power received by the reader is only 20 dB higher than the sensitivity of the reader. This margin can be easily lost, if the transmitter noise couples to the receiver. Hence reader architecture is also important, especially because the transponders are becoming ever more sensitive with the introduction of semi-passive transponders.

The chips usually use a low modulation factor, such as the measured value $m$ = -16 – -6 dB [41]. It can also be seen that modulation indexes smaller than $m = -6$ dB do not significantly affect the range. Because small modulation indexes are typically used in UHF RFID, the unmodulated

effective aperture can be used in Eq. (2.18), which gives the form

$$r_{max} = \frac{\lambda}{4\pi}\sqrt{\frac{G_{tag}G_{tx}P_{tx}}{P^0_{tag}}\tau}, \tag{2.20}$$

where $\tau$ is the mismatch term

$$\tau = \frac{4R_AR_L}{(R_A+R_L)^2+(X_A+X_L)^2}. \tag{2.21}$$

The mismatch term can have values $0 \leq \tau \leq 1$. Equation (2.20) is often referred to as the read range equation for UHF RFID.

## 2.7 Millimetre Wave Identification

What if the carrier frequency RFID was at the millimetre waves? The idea of RFID at millimetre waves was first proposed in [61] and analysed in more detail in [II]. Before that, the highest frequency used for RFID was 24 GHz by Biebl [62].

The main differences between the RFID and MMID systems is the wavelength, which scales the effective aperture and the radar cross section. MMID also enables communication at higher data rate, because a wide bandwidth is available e.g. at 60 GHz.

At millimetre waves small antennas can give very high gain. However, this cannot be used to increase the gain of the transponder, as this makes the transponder only accessible from the main beam direction — a direction that is not known in many applications. Thus the transponders use a low-gain antenna.

The read range of MMID at 60 GHz is graphically analysed in Fig. 2.5 (see Errata), which suggests that passive operation is limited to the centimetre range by power transfer to the transponder. On the other hand, the signal-to-noise ratio at the receiver is very high at the low distances, allowing the widening of the data (and noise) bandwidth. Even gigabit data transfer would be possible to a distance of a few cm, which could be used in wireless passive mass memories. Of course, low directivity antenna is required also for the reader to satisfy the far-field criterion for the Friis equation.

In [II] also semi-passive MMID is discussed. Its range is limited by the reader sensitivity, which would allow a range of a few meters, as seen from

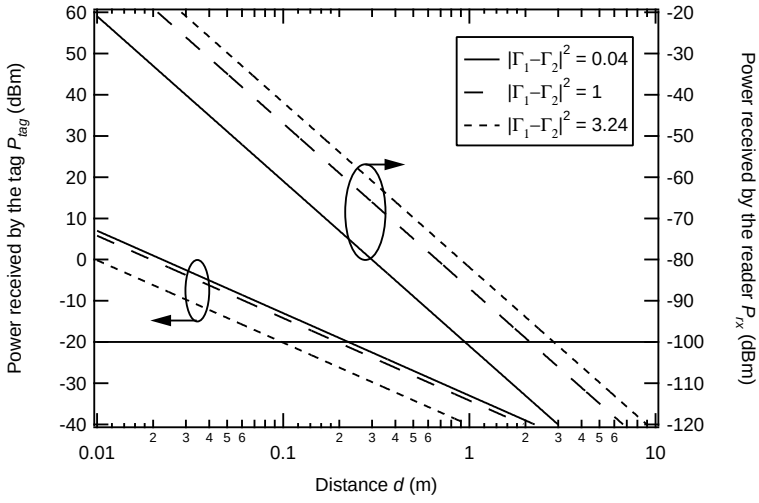


*Figure 2.5. The limiting factors on the MMID range at 60 GHz with $G_{tx}P_{tx}$ = 2 $W_{erp}$, $G_{rx}$ = 20 dBi, $G_A$ = 0 dBi [II].*

Fig. 2.5. This enables an application similar to today's RFID, where an ID code is transferred over a few meters. The narrow-beamed antenna of the MMID reader could deliver pinpoint accuracy in the localisation of the transponders, which is not possible with UHF RFID.

An active MMID could deliver a range of a hundred metres. This could be used in road environment, where automotive radars could be used as readers [II]. The radars already have all hardware required.

Figure 2.5 presents only one possible configuration for the MMID system. The range can be extended by more sensitive transponders, higher gain antennas, etc. The backscattering modulation is verified in [II] at 60 GHz and in [63] at 77 GHz. The spectrum of a modulated backscattered signal is shown in Fig. 2.6. Even though the bandwidth of the measurement is small, the measurement proves that MMID can be implemented with a better transponder modulator and a more sensitive reader device.

## 2.8 Limitations of the Free-Space Model

The range equation (Eq. (2.20)) was derived for ideal free-space conditions. A multitude of unidealities effect the performance of the RFID system in real-life situations, which will now be shortly commented.

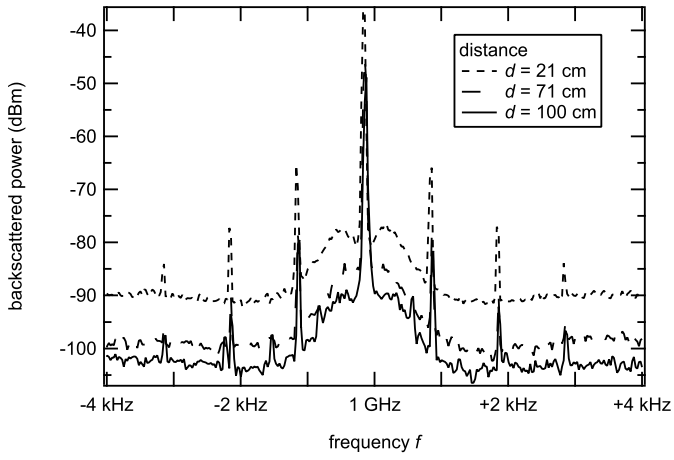


*Figure 2.6. Measured backscattered spectra. Resolution bandwidth is 100 Hz and the data has been averaged over 100 samples [II].*

First of all, Eqs. (2.18) and (2.19) are valid in the far field, usually defined by the criterion $d > 2D^2/\lambda$, where $D$ is the greatest dimension of the antennas [43]. At UHF the reader antenna is usually a $\lambda/2$ -patch. Hence the far field criterion can be written as $d > \lambda/2 \approx 18$ cm.

*Transmitter Noise*

The transmitted signal couples to the receiver through the near-field of the reader antenna and through environmental reflections. The attenuation in the coupling can be as low as -20 dB – -30 dB. The transmitted signal carries amplitude and phase noise originating in the oscillator and the power amplifier, which can then dominate over the noise generated at the receiver. The high sensitivity of the reader, which was used in the range analysis, requires high isolation between the transmitter and the receiver. This will be further discussed in Chapter 4.

*Mismatch*

The read range analysis assumed ideal backscattering modulation, where $\Gamma_1 = -\Gamma_2$. This implies best possible power matching between the antenna and the load. Good matching is even more important than usual: Increasing the mismatch deteriorates the backscattering modulation faster than it diminishes the power transfer. Measurements of the effect are presented in Fig. 2.7.

A typical source of mismatch is a change in the environment within the near-field of the transponder antenna. In general, a change in the

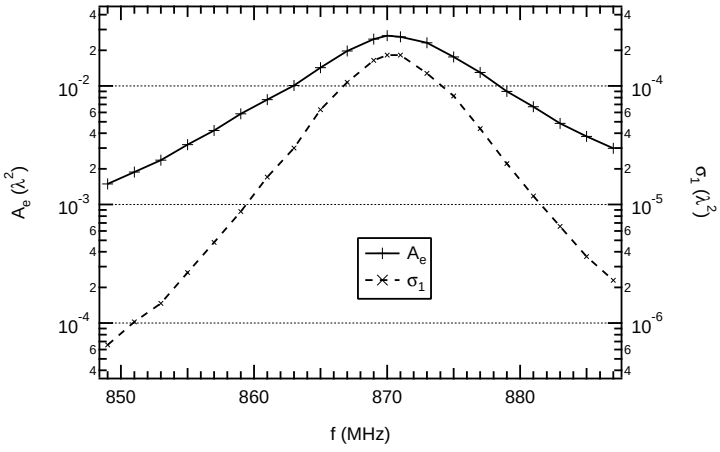


*Figure 2.7. The measured aperture $A_e$ and radar cross section $\sigma_1$ of a transponder in free space [IV].*

antenna surroundings effects the antenna input port impedance. The effect is discussed in Chapter 3.

*Fading*

When the environment is full of reflectors and scatterers, signals arrive at the same point via different paths. This multipath propagation leads to interference. The destructive interference creates areas of diminished RF field. In simple geometries, the areas of diminished field can be calculated, but in practice this is impossible. Hence measurements and statistical fading analysis must be used. The fading effect is considered in more detail in [41] and measurements on fading in backscattering communication at 2.45 GHz can be found in [64].

*Polarisation*

The power transfer and the received scattered power are affected by the transponder and reader antenna polarisations. At UHF, usually linearly polarised transponder antennas and circularly polarised reader antennas are used. This ensures operation regardless of polarisation, but introduces a polarisation loss of $p = -3$ dB. The polarisation loss is a function of the polarisations and inclinations of the reader and transponder antenna [41].

The polarisation loss can be taken into account in the range analysis by replacing the transponder antenna gain $G_A$ by the term $pG_A$. Hence the loss will affect power transfer in the first and the radar cross section in the second order. In the range equation the polarisation mismatch term is found under the square root.

## 2.9 Summary

In this chapter, the fundamental equations for the powering of the transponder and the communication by backscattering modulation have been discussed. The equations have been applied to passive UHF RFID, whose range was shown to be limited by the power transfer, if the reader sensitivity is not deteriorated by the transmitter noise. The analysis was also applied to millimetre wave RFID, or MMID. Experimental verification of the theory at 60 GHz was also presented.

A review of the integrated circuits of the UHF transponders, as well as reader circuits was presented. As far as the author is aware of, the sensor IC presented in the Thesis is the only published IC with an ADC for external sensors. The chip provides a 10 bit ADC with a power consumption of 30 $\mu W_{DC}$, which is in the same order of magnitude than other sensor ICs with a 10 bit ADC.

# 3 Transponder Antennas

This chapter takes a closer look at the transponder antennas. First the antenna scattering is further discussed. The more thorough treatment of the antenna scattering reveals possibilities for characterising the transponder antennas by their scattering. Two measurement techniques are presented. Finally, transponder antenna requirements are discussed, and a transponder antenna design is introduced and compared with other published transponder antennas.

## 3.1 Backscattering from Antennas

King [21] and Harrington [22] developed a general antenna scattering theory from a general linear three-port model. The three ports describe the input ports of a transmitting (subscript $tx$), receiving (subscript $rx$) and scattering (subscript $a$) antennas. By writing a three-port impedance matrix for the system and assuming that the scattering antenna port's current and voltage satisfy Ohm's law with the load impedance $Z_L$, an equation for the received signal can be written as

$$V_{rx} = \left( Z_{rx-tx} - \frac{Z_{tx-a} Z_{rx-a}}{Z_D + Z_L} \right) I_{tx}, \tag{3.1}$$

where $Z_D$ is the input impedance of the scattering antenna. According to the Eq. (3.1), the scattering can be considered to consist of two parts: the structural mode scattering (the first term), and the antenna mode , or re-radiated, scattering (latter term). The structural mode scattering does not depend on the antenna load, and the antenna mode scattering is load-dependent.

The definitions of the structural and antenna mode scattering are ambiguous. In practice they cannot be distinguished from each other by measurements. Equation (3.1) would suggest that the structural mode scatter-

ing can be measured by attaching an open load to the scattering antenna port. However, several other definitions are used in the literature. Sometimes the structural mode scattering refers to short-circuit scattering, at other times to scattering with a matched load [65]. In this thesis, the structural scattering refers to the scattering with an open load, as suggested by Eq. (3.1). This definition is also used in [V].

Equation (3.1) is derived for a general antenna, only assuming a linear three-port model with a linear load, and it holds for all kinds of antennas. In the previous chapter, the equivalent model of Fig. 2.2 leads to a similar equation for the current in the circuit, namely the Eq. (2.5).

However, compared to Eq. (3.1), Eq. (2.5) describes a special case, where the structural scattering term $Z_{rx-tx} = 0$. The equivalent model in Fig. 2.2 describes a minimum scattering antenna, which is defined as an antenna that scatters as much power as is transferred to the load, when connected to a matched load [65]. From this definition it follows, that with an open load, the antenna does not scatter any power. Yet the definition requires that the antenna scatters with the same pattern as it radiates.

The definition of a minimum scattering antenna seems very restricting, but it turns out to be very useful. For example, electric dipoles are minimum scattering antennas. Other common RFID transponder antennas, such as the patch and planar inverted-F antenna (PIFA), are not minimum scattering antennas, especially as they may scatter in different modal distributions, i.e. with different pattern than they radiate [65, 66]. However, the analysis presented in the previous chapter can be used to describe the modulated backscattering from all types of antennas. In [67], the antenna mode scattering, which is affected by the load, is derived independently of the model of Fig. 2.2. The result is similar to Eq. (2.5). Further the modulated radar cross section $\sigma_m$ in Eq. (2.15) does not contain the structural mode scattering term, but is only a function of the difference of the antenna mode scattering with different loads [68]. Hence, $\sigma_m$ of Eq. (2.15) is valid for all antennas, but $\sigma_0$ of Eq. (2.12) holds only for minimum scattering antennas.

## 3.2 Measurement of Transponder Antennas

A design goal of a transponder antenna is the maximisation of the mismatch term $\tau$ in the read range equation (2.20). In principle, the mismatch can be measured by connecting a feed line to the antenna feed port and

measuring the reflection with a network analyser. However, the transponder antennas are very small, and the feed line cannot be efficiently isolated from the antenna radiation and near fields. Hence, the feed line inevitably affects the antenna radiation pattern, and input impedance. The coupling effects are complicated, and the antenna impedance cannot be simply deembedded from the measured results. Some antenna structures, such as a dipole antenna, allow a symmetric feed line to be attached perpendicular to the electric fields, which the antenna generates. In these cases, accurate measurements can be carried out, but with a more complex antenna structure this is not possible.

The integrated circuits (ICs) of the transponders have a capacitive input impedance (see Table 2.1). The matching elements required for direct matching to the capacitive IC are incorporated into the antenna, making the input impedance of the antenna highly inductive, which leads to a high reflection from a 50-ohm feed line. In addition to this, it is not always clear, whether the antenna should be fed with a single-ended (referred to ground) or a symmetric signal, as in the case of the PIFA presented in [III]. These unique properties of the transponder antennas tend to increase the feed line radiation, and hence diminish the accuracy of feed line measurements.

In [IV] the antenna radiation pattern is measured with the backscattering and feed line methods, and the result is compared with simulations. It is clearly seen, that the radiation pattern of a small antenna is badly distorted in the feed line measurement — even though a matching circuit and an optical feed are used.

The backscattering from transponder antennas is discussed and measured in [69], but the scattering has not been used to characterise the antenna power transfer or input impedance. The feed line problem has been solved in [70] by contactless near-field measurement of the radiation pattern. Also commercial devices for wireless measurements of RFID transponders are available. The devices can measure both the power transfer and the received backscattered power, see e.g. [71].

In this Thesis two scattering-based techniques for measuring the mismatch term are presented. In [IV] and [72] a method for measuring the effective aperture expressed in Eq. (2.7), effectively measuring the power transferred to the load of the antenna. The technique presented in [V] relies on Eq. (3.1) to measure the input impedance of the transponder antenna, from which the mismatch term $\tau$ can be calculated.

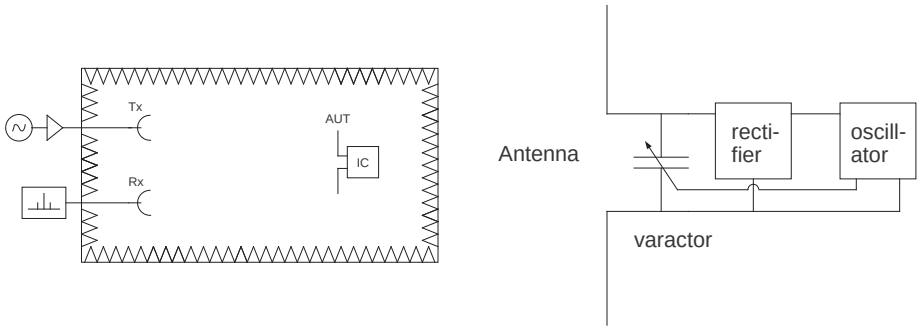


*Figure 3.1. Aperture measurement. The measurement setup (left) and the block diagram of the antenna – chip system (right) [IV].*

## 3.3 Power Transfer

In [IV], the antenna under test (AUT) is connected to an IC chip that has a low-frequency oscillator inside it, as shown in Fig. 3.1. The power for the operation of the oscillator is generated from the incident RF power. The oscillator drives a modulator at the input of the chip, causing backscattering modulation, which is seen as sidebands in the scattered signal.

The chip is designed so that the RF power $P_{rf,0}$ necessary for its operation is known. The Friis equation can now be written in the form [IV]

$$A_e = \frac{P_{rf,0}}{S_{ref}} \frac{P_{tx,ref}}{P_{tx,0}}. \tag{3.2}$$

First, the reference power intensity $S_{ref} = S(P_{tx,ref})$ is measured with a transmission power of $P_{tx,ref}$ by placing a reference antenna at the location of the AUT. Then the reference antenna is replaced by the AUT, and transmission power is slowly ramped up at the transmitter. When the power transferred to the IC reaches $P_{rf,0}$, the load modulation begins, and sidebands appear at the receiver. The lowest transmit power that wakes the sidebands is the critical transmit power $P_{tx,0}$.

Equation (3.2) provides a procedure to measure the antenna aperture, and hence the mismatch term $\tau$. The measurement is simple and robust, because the scattered power levels are not needed to calculate the result. Equation (3.2) can be used to measure antenna radiation patterns and bandwidth.

In [IV], the measurements of a PIFA-type antenna [III] are carried out in

free space and on two different sizes of metal platforms to study the effect of the mounting platform. The radiation patterns are presented in Fig. 3.2 and compared with simulations (Fig. 3.3) and feed line measurements (Fig. 3.4). The feed line is connected to the PIFA through the metal platform, so that the platform shields the antenna from feed line coupling. The results of the aperture measurement (Fig. 3.2) comply with the simulations (Fig. 3.3) with all the sizes of the metal platform, but the smaller the platform, the worse the results of the feed line measurement (Fig. 3.4).

The bandwidth measurement gives direct information on the mismatch term $\tau$. The measured effective aperture of the PIFA is presented in Fig. 3.5 as a function of frequency. The reactive part of both the IC and the antenna change fast as a function of the frequency, whereas the real parts are almost constant. Hence, the measurement result shown in Fig. 3.5 can be considered to present the reactive mismatch in the term $\tau$. The measurement helps to identify the frequency, at which the reactive mismatch is at its minimum, but cannot be used to measure the resistive mismatch, as the measured effective aperture consists of the product of the antenna gain and the mismatch term. Hence, the absolute value of the aperture at its maximum is also the product of these two terms, and the magnitudes of those cannot be extracted from this measurement only.

Figure 3.5 shows the measured aperture at three different mounting platforms. As an example, the aperture is 3 dB greater on a big metal plate than in free space. It would be tempting to state that this is due to the change from an omnidirectional (free space) to a hemispherical (metal) radiation pattern, but the effect could also be due to a change in antenna input impedance. Without further measurements, the effects cannot be distinguished.

Despite its limitations, the aperture measurement gives direct information on the antenna behaviour with the correct loading, and in an actual application environment. The method is robust, and the measurements can be carried out in a normal laboratory environment, or in an RFID application environment. The measurement method has been found useful, not only by the author, but also by other RFID antenna developers, who have used the method developing several antenna structures, e.g. [73, 74, 75].

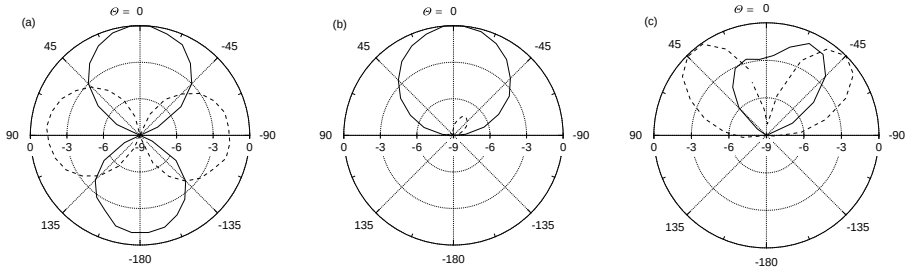


*Figure 3.2. The radiation patterns of the PIFA measured with the aperture method: (a) in free space, (b) on (150 mm)$^2$ metal and (c) on (600 mm)$^2$ metal. The solid line (—) denotes the co-polarisation and the dashed line (- -) the cross-polarisation [IV].*

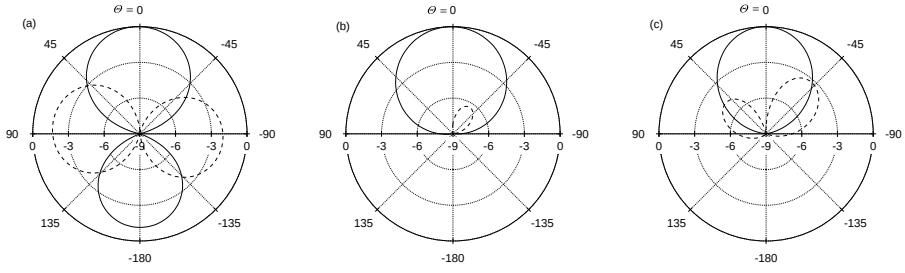


*Figure 3.3. The radiation patterns of the PIFA simulated with HFSS: (a) in free space, (b) on (150 mm)$^2$ metal and (c) on infinite metal. The solid line (—) denotes the co-polarisation and the dashed line (- -) the cross-polarisation [IV].*

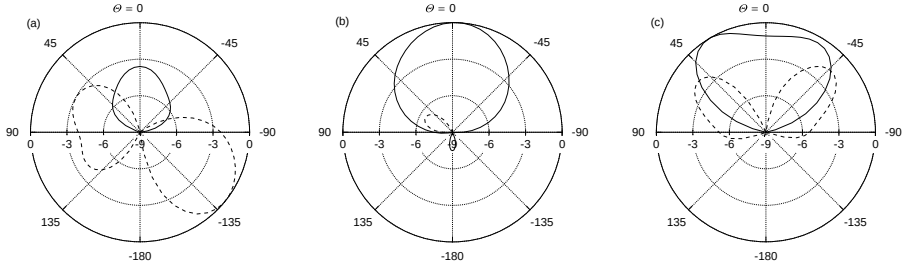


*Figure 3.4. The radiation patterns of the PIFA measured with the feed line method: (a) in free space, (b) on (150 mm)$^2$ metal and (c) on (600 mm)$^2$ metal. The solid line (—) denotes the co-polarisation and dashed line (- -) the cross-polarisation [IV].*

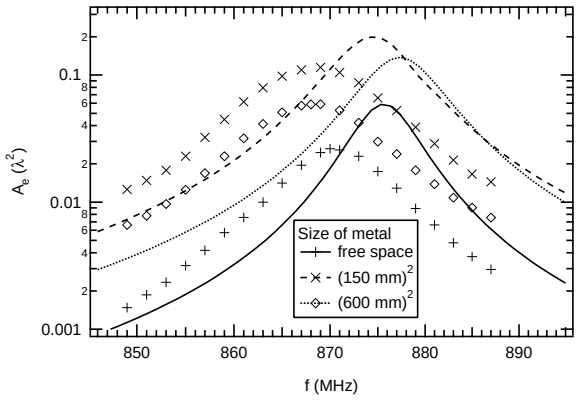


*Figure 3.5. The measured (markers) and calculated (lines) apertures of the PIFA on different platforms as a function of frequency [IV].*

## 3.4 Input Impedance

To obtain information on both the resistive and reactive mismatch, Eq. (3.1) can be used to measure the input impedance $Z_D$ of the antenna. This approach is a more conventional one. While the author has not seen the aperture of the antenna measured earlier as presented in [IV], a multitude of other antenna measurement methods based on the backscattered field have been reported.

Already in 1963, Harrington proposed the use of active loads to measure field strengths by backscattering [23]. In 1979, Appel-Hansen [24] presented a method for antenna gain measurement. He used short-circuited transmission lines of different lengths as the load of the AUT. Mayhan et al. [25] presented a method for measuring the antenna input impedance in 1994. Wiesbeck and Heidrich [26] went a step further in 1998 by measuring the whole scattering matrix of an antenna with two radiation (both polarisations) and several load ports.

The technique presented in [V] is an extension of the method developed by Mayhan et al. in [25], who considered only real antenna load impedances. But because the transponder antenna input impedance is highly inductive, it is necessary to use capacitive loads. In [V], the theory is expanded for reactive loads, and measurements of two transponder antennas are presented.

Equation (3.1) has four unknown parameters, but it describes bistatic scattering, i.e. separate transmission and receiving antennas are used. In monostatic case, the terms $Z_{tx-a}$ and $Z_{rx-a}$ are equal. Hence, measurement

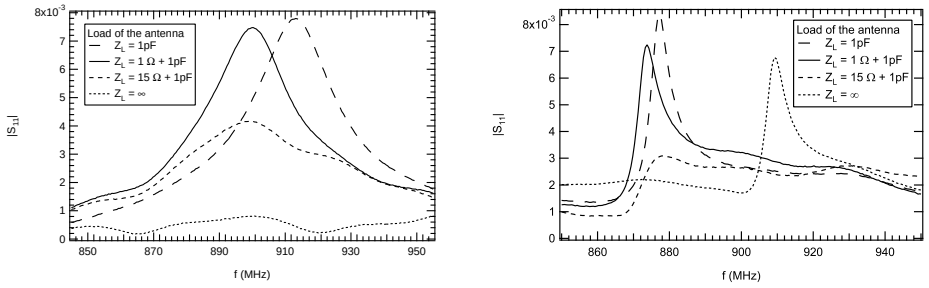


*Figure 3.6. The measured scattering parameters $S_{11}$ with different loads of the Palomar antenna (left) and the PIFA (right) [V].*

of the scattering with three known loads gives a group of three equations with three unknowns. The solution for the input impedance is [V]

$$Z_D = \frac{Z_m - AZ_c}{A - 1}, \tag{3.3}$$

where $A$ contains the measured scattered fields

$$A = \frac{S_c - S_o}{S_m - S_o}. \tag{3.4}$$

The used loads $Z$ (and the respective measured scattered fields $S$) are: open load $Z_o = \infty$ ($S_o$), capacitive match $Z_c \approx -jX_A$ ($S_c$) and conjugate match $Z_m \approx R_A - jX_A$. The result reduces to the one given in [25], if capacitive match is taken to be a short circuit ($Z_c = 0$) and $Z_m$ is purely resistive.

Equation (3.3) has three noteworthy aspects. First, the equation does not include any coupling constants from the measurement apparatus to the antenna, and only linear coupling is assumed. Therefore the measurements can be carried out in free space as in [25], or in a gigahertz transverse electromagnetic mode (GTEM) cell [76], [V]. Further, the scattered fields only appear as a ratio of two differences in the equation. Hence, a simple background reduction from every scattered field does not affect the results, if the background remains constant over the measurement. Finally, the equation does not take into account polarisation coupling in the AUT. Most antennas have two orthogonal radiation ports, i.e. two polarisations are radiated. Accurate results are only to be expected in the case of antennas, where one of the polarisations is highly dominant, such as electric dipole.

The two antennas measured in [V] are the Palomar antenna [32], an electrical dipole in a spiral, and a PIFA similar to the one described in [III]. The scattered fields of the antennas with several loads are presented in Fig. 3.6.

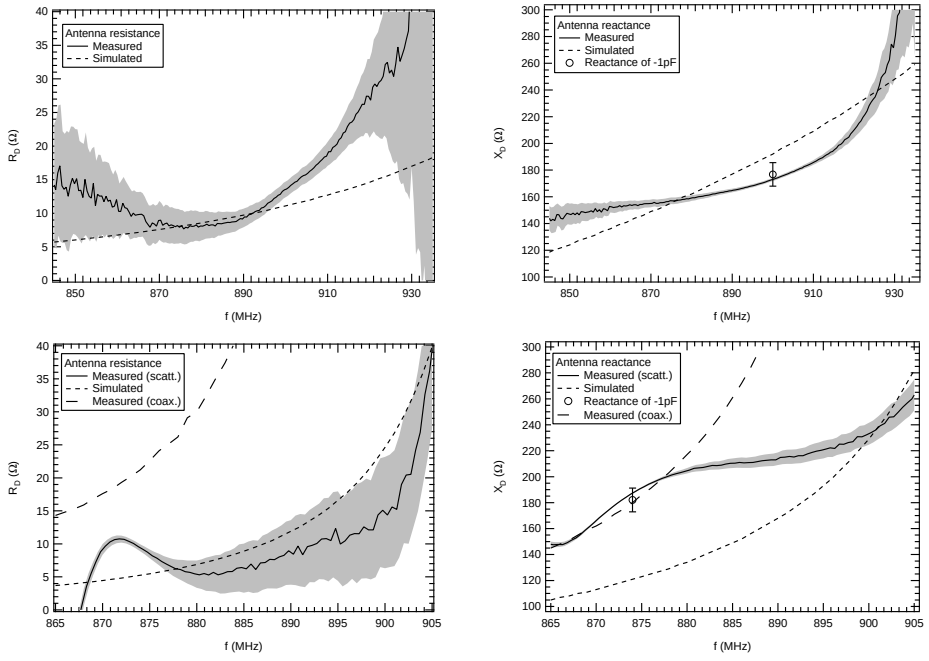


*Figure 3.7. The measured and simulated input impedances $Z_D = R_D + jX_D$ of the Palomar antenna (above) and the PIFA (below). The grey area represents the uncertainty in the measured value [V].*

The model in Fig. 2.2 suggests that a short-circuited antenna would scatter a fourfold power compared with the matched antenna. Fig. 3.6 shows that an approximately twofold scattered field is detected from the short-circuited antenna compared with the matched case. This, again, justifies the model used in Chapter 2.

Figure 3.7 presents the input impedance results for the two antennas. The grey area in the figure represents the random uncertainty derived in [V]. The error arises from residual background scattering and displacement error, and is a strong function of the reference loads. The optimal choice of the reference loads is considered in the error analysis in [V]. The error is found to be the smallest when reactive matching is the best, which is also seen in Fig. 3.7. Hence, all the loads have capacitive matching. The resistive loads are to be chosen far apart, i.e. an open, a matched and a shorted load.

The results are in a good agreement with the simulations and the feed line measurements in the case of the dipole. The results of the PIFA are reasonable in the immediate neighbourhood of the resonance peak, but clearly unphysical farther away from the peak. The PIFA radiates a significant

amount of power to the other polarisation, which is not measured, and not considered in the simple model, which the analysis is based on. Hence, a systematic error is to be expected.

The measurement technique is reliable when measuring electrical dipoles and other antennas that have a single dominant polarisation. The electrical dipoles present a major proportion of the RFID transponder antennas. However, when the antennas radiate a significant amount of power to both polarisations, the results are only indicative. In such a cases, both polarisations should be measured and the analysis developed further.

## 3.5 Transponder Antenna Requirements

All transponder antennas in RFID applications need to satisfy three main requirements: 1) The antenna must have a simple structure that is mass-producible with low cost; 2) the tag must be small in size; and 3) it must (in its own part) provide long read range. The design process and considerations for transponder antennas are well summarised in [77].

In general, there are two types of antennas are on the market. First, labels that usually employ an electric dipole. The dipole is easy to manufacture with a roll-to-roll process using only one metallisation layer on a thin plastic foil. The antenna and matching elements are patterned to the same metallisation layer for direct match to the capacitive RFID IC. This makes it possible to manufacture very low cost transponders, even less than 10 Euro cents. Second, there are antennas that have at least two metal layers. Typical designs are a patch, a planar inverted-F antenna (PIFA), and an electric dipole on a metal plane. The antennas can be attached to metal and other surfaces, and they often have a robust casing. Both the more complex antenna structure and the sturdier casing make the antennas more expensive, typically a few Euros. These antennas are often called platform tolerant, universal, or metal-mount transponders.

Independent of the antenna structure, the low form factor required implies low directivity of the transponder antenna. This seems to lower the read range according to Eq. (2.20), but actually helps to increase the read reliability in many applications. Usually the transponder location and orientation cannot be accurately known. Hence a high-gain, narrow-beam transponder would be hard to access, because the main beam direction is not known. Hence, low-gain transponders are suggested also for MMID applications [II].

The third requirement basically implies low loss and good matching to the IC. The second and third requirements are closely related, because the antenna size limits the gain and the bandwidth of the antenna: The smaller the antenna, the narrower the band and lower the gain [78, 79].

## 3.6 Platform Tolerance

One-layer electric dipoles are very sensitive to their immediate surroundings, i.e. the dielectrics and conductors in their near field. The dielectrics and metals detune the antenna. When the resonance shifts from the desired frequency, the input impedance of the antenna changes. The detuning affects both real and imaginary parts of the input impedance. Hence, the mismatch term $\tau$ in the range equation (Eq. (2.20)) decreases, diminishing the read range. The effect can be very strong, making it practically impossible to read the transponder at all. The detuning has been studied and measured e.g. in [80, 81].

The antennas with two metal layers are less sensitive to the electric properties of the materials near the antenna, especially to the material of the mounting platform. The antennas are not detuned, and their input impedance is not influenced by the mounting platform. This is called platform tolerance.

The effect of the mounting platform on the transponder antenna has been found to be crucial to the success of UHF RFID since at least 1999, when Foster [82] concluded that narrow-beamed antennas are preferable in order to achieve better isolation from the mounting platform. However, also the near field of the antenna couples to the mounting platform. The whole current distribution of the antenna must be taken into account when studying the effect of the mounting platform [83, 84].

The mounting platform of the antenna also affects the radiation pattern, especially on metal platforms. However, the detuning usually has the stronger effect on the read range. The change in the radiation pattern has been measured in [85] for electrical dipoles and in [IV] for a platform tolerant PIFA.

The PIFA presented in [III] is one of the first published platform-tolerant antennas. Due to the interest on the research field, it has also been very widely referenced to. Later structures that offer better platform tolerance are published, but the read range achieved from the metal surface was unprecedented in 2004. The structure of the PIFA is presented in Fig. 3.8. It contains only two metal layers and two contacts between them.

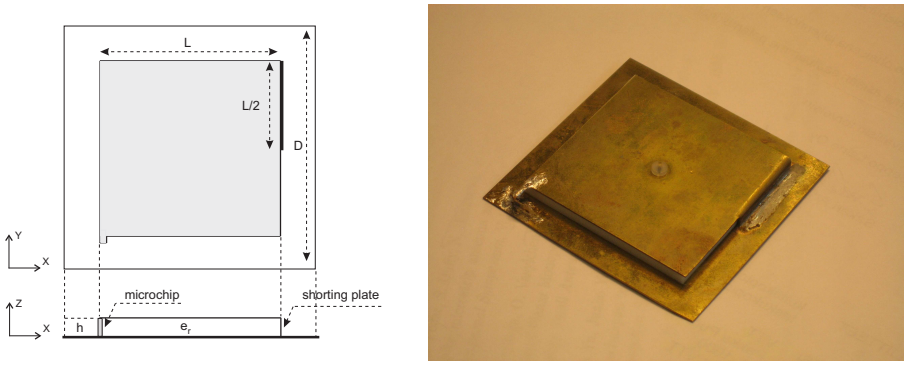


*Figure 3.8. The structure (left) and photograph (right) of the PIFA: $D$ = 59 mm, $L$ = 45 mm, $h$ = 3 mm, and $\varepsilon_r$ = 2.1 (Teflon) [III].*

## 3.7 Overview of Platform-Tolerant Antennas

Numerous transponder antenna structures have been published. In this section, a review of published platform-tolerant transponder antennas is presented. The review includes antennas published in peer-reviewed journals, some of which are commercialised. A transponder that is commercialised, but not published, is included in order to give an example of a dipole-on-metal transponder [86]. The overview is summarised in Table 3.1.

Platform-tolerant antennas have three basic structures: a dipole on a ground plane, a patch, and a PIFA. The comparison of the antennas is complicated, because different transponder ICs and radio regulations are used in the publications. Comparing only antenna gains is not relevant either, because impedance matching is the key issue. The difference of the read ranges on different platforms describes the platform tolerance, and wider band ($\Delta f$) antennas lend themselves better to mass production. The absolute read ranges in particular cannot be directly compared between the transponders, because the transmission power and other components of the system, e.g. the reader and the transponder sensitivity, strongly affect the result.

Low-profile antennas tend to be narrow-banded. The bandwidth can be increased using a dual resonance [87, 88]. The same technique has been used in [89] to achieve a dual-band operation. The commercialised transponders [86, 88] have a higher bandwidth than the other transponders.

The use of metamaterials, like electronic band gap structures (EBGs) and artificial magnetic conductors (AMCs) have been widely studied [90,

*Table 3.1. Review of metal-mount transponders.*

| Read Range (m) metal | free space | TX Power | $\Delta f$ (MHz) | $f_0$ (MHz) | $Z_L$ ($\Omega$) | IC | Structure | Size ($mm^3$) | Ref | Year |
|---|---|---|---|---|---|---|---|---|---|---|
| 4 – 5 | 2 | 0.5 $W_{erp}$ | 15 | 869 | 7-$j$170 | Tagidu | PIFA | 59 × 59 × 3 | [III] | 2004 |
| 1.0 | 0.5 | — | — | 915 | 1200 | — | IFA | 200 × 160 × 10 | [93] | 2004 |
| 1.9 | 1.5 | — | — | 915 | 1200 | — | Patch, EBG | 100 × 100 × 6.4 | [90] | 2004 |
| — | — | — | 57 | 915 | 6-$j$125 | — | Patch | 74 × 24 × 3 | [87] | 2006 |
| 10 | 7 | 2 $W_{erp}$ | 13 | 867, 915 | 10-$j$160 | Tagidu | PIFA | 62 × 51 × 3 | [89] | 2006 |
| 4.8 – 5.2 | 6 | — | 27 | 915 | 15-$j$140 | Alien AL-9238 | Patch | 86 × 50 × 5 | [73] | 2006 |
| 4.5 – 4.9 | 5 | — | 26 | 915 | 6.2-$j$127 | Alien ALN-9338-R | shorted Patch | 50 × 47 × 3 | [74] | 2007 |
| — | — | — | 10 | 900 | 12-$j$300 | Philips | dipole, AMC | 100 × 100 × 5 | [91] | 2007 |
| 3.5 – 4.2 | 2.7 | — | 26 | 915 | 14.3-$j$62 | TI | Patch | 80 × 40 × 1.6 | [75] | 2008 |
| 4 | 2.5 | 4 $W_{eirp}$ | 100 | 915 | 40-$j$120 | Impinj EPC Gen2 | Patch | 79 × 31 × 10 | [88] | 2008 |
| 8.5 | 7 | 4 $W_{eirp}$ | 100 | 915 | 40-$j$120 | Impinj EPC Gen2 | Patch | 155 × 32 × 10 | [88] | 2008 |
| 6.0 | 4.2 | 2 $W_{eirp}$ | 12 | 910 | 6-$j$125 | Alien EPC Gen2 | dipole, AMC | 121 × 34 × 3.5 | [92] | 2008 |
| 5 – 7 | | — | 100 | 910 | — | Impinj/NXP EPC Gen2 | dipole on metal | 224 × 24 × 8 | [86] | — |

91, 92]. The structures include at least three metal layers. Table 3.1 does not indicate any significant performance improvement due to the use of metamaterials. The reason is that the transponders must be small, but the EBG and AMC ground planes require a size of several wavelengths to work properly [91].

## 3.8 Summary

In this chapter, the development and measurement of transponder antennas was discussed. Two backscattering-based measurement techniques were presented, and the antenna scattering studied with the techniques. The backscattering-based measurements give better results than feed line measurements, because near-field of the small antenna couples to the feed line.

A platform-tolerant PIFA antenna for the transponder was presented, and compared with other antennas found in the literature. The PIFA was one of the first published platform-tolerant antennas. When published, it provided an unprecedented read range on metal.

# 4 RFID Reader

Most radio devices used daily in modern society are transceivers, i.e. they include both a transmitter and a receiver, but usually the receiver and transmitter signals are isolated by multiplexing. Possible physical multiplexing schemes are frequency (FDM) or time division multiplexing (TDM), and several digital multiplexing schemes also exist, like the code division multiplexing (CDM). For example in GSM, both FDM and TDM are used. The transmitter and receiver have separate frequency ranges with about a hundred channels (FDM), and each frequency channel is divided into random time slots to allow multiple user within a single channel (TDM). The physical multiplexing schemes efficiently isolate the transmitter and receiver signals, allowing the receiver and transmitter modules to be independently designed and implemented.

Physical multiplexing cannot be used to isolate the receiver and transmitter signals in passive RFID. Even though the data transfer in RFID is time-division multiplexed, i.e. the reader and the transponder do not send data at the same time, the reader has to be sending a continuous wave (CW) signal, when the transponder is sending, since the transponder uses the CW signal from the reader to power itself, and as a carrier for the backscattering modulation.

The fact that the receiver is used simultaneously at the same frequency as the transmitter has its drawbacks, but also benefits [VI, VII]. The obvious drawback is the requirement for high dynamic range in the receiver [46]. The received signal is as low as -70 dBm, but the transmitter signal up to +36 $\mathrm{dBm}_{eirp}$ can have as high a coupling as -20 dB to the receiver. The high power of the incident carrier can saturate the receiver. The incident carrier also carries the transmitter noise into the receiver. To minimise these effects, high isolation between the transmitter and the receiver is required.

Most RFID receivers have a direct conversion detector. Because the transmitter and the receiver are co-located, the transmitted ($tx$) signal is generated from the same local oscillator ($lo$) that is used for downmixing

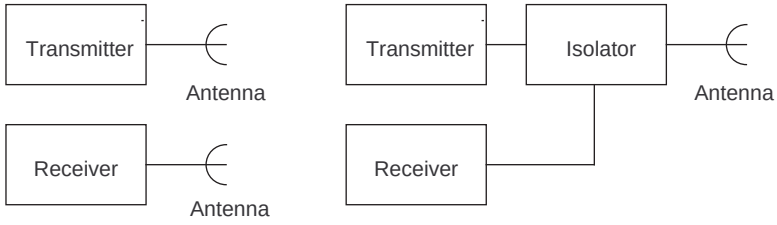


*Figure 4.1. Principal architectures of a bistatic (left) and a monostatic (right) reader.*

the received ($rx$) signal. Because the radio path is short compared to the modulation wavelength, $\lambda_m = 2\pi c/\omega_m$, the noises of the $rx$ and $lo$ signals are at least partially correlated, which may actually help to increase the dynamic range. The phenomenon is called range correlation [94].

The RFID reader can be realised mono- or bistatic (Fig. 4.1), i.e. having a single or separate antennas for transmitting and receiving. If monostatic architecture is used, the RF front end needs an isolator between the transmitter and the receiver. Common isolation techniques include a circulator and a directional coupler, or else an adaptive front end can be used. The adaptive RF front end adds an additional compensation signal to the input of the receiver. The feedback from the receiver keeps the amplitude of the compensation signal is equal and the phase opposite to the incident carrier. These isolation techniques are presented in Fig. 4.2 for a monostatic reader.

## 4.1 Isolator Review

The common isolation techniques in case of the RFID reader have been described in [41, 95]. The circulator can provide up to -30 dB isolation, but the antenna reflection loss is rarely below -20 dB, which limits the isolation to -20 dB, too. A weakly coupled directional coupler can deliver up to -40 dB isolation with ca. -10 dB reception loss [96]. Separate antennas for transmission and reception can give -30 dB isolation, but is inconvenient in practice.

Because these common isolation techniques do not provide a sufficient solution in an RFID reader, the issue has been widely studied in the recent years. The research falls in two categories. On the other hand, the isolation of a directional coupler has been increased [96, 97, 98, 99], and on the other hand adaptive RF front ends have been designed [100], [VI, VII].

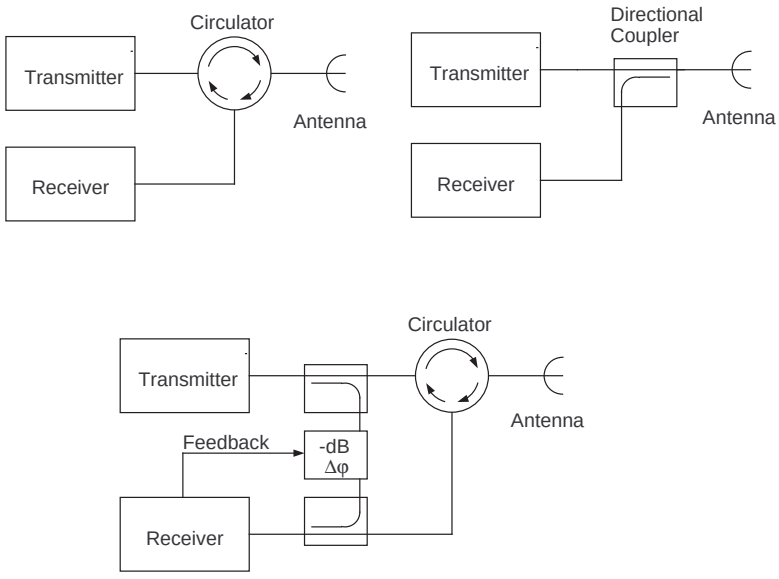


*Figure 4.2. Common isolation techniques for the RFID reader front end: a circulator (above left), a directional coupler (above right), and an adaptive front end (below).*

Additionally, an antenna including a hybrid to provide the isolation has been suggested in [101]. The review of the published isolator elements is summarised in Table 4.1.

The directional couplers provide -45 – -60 dB isolation with -11 – -15 dB coupling. The high isolation is achieved by choosing the load in the matched port of the coupler according to the antenna impedance [97, 98, 99], but it is not reported, how the impedance is realised or varied. If the matched port impedance is not adaptive, the isolation will diminish, if the antenna impedance is changing. Especially in hand-held devices, the antenna impedance will vary due to the user hand moving in the antenna near-field.

This Thesis introduces two truly adaptive RF front ends. In [VII], an adaptive RF front end for mobile devices is presented. The front end is considered to be a impedance measurement bridge, which is very similar to the idea of using a directional coupler and a tunable load. The coupler achieves a -50 to -60 dB isolation with a -7 dB coupling.

The adaptive RF front end presented in [VI] is similar to the circuit in [100]. The papers were published independently of each other at the same time. The design used in [VI] is based on a patent filed in 2005 [102].

*Table 4.1. Review of Isolators.*

| $f_0$ (MHz) | $L_{tx-rx}$ (dB) | $L_{tx-ant}$ (dB) | $L_{ant-rx}$ (dB) | $F$ (dB) | $P_{1dB}$ (dBm) | Size (mm) | Adaptive | Ref | Year |
|---|---|---|---|---|---|---|---|---|---|
| 860 – 960 | -64 | — | -15 | — | — | 58 × 34 | No | [97] | 2006 |
| 860 – 960 | -36 | 8 | 8 | — | — | 450 × 200 × 30 | No, incl. antenna | [101] | 2006 |
| 912 | -45 | — | -11 | — | — | 1.5 × 1.5 | No | [96] | 2007 |
| 865 – 869 | -50 | -3 | - 7 | 12 | — | 40 × 40 | Yes | [VII] | 2008 |
| 920 | -65 | — | -10.5 | — | — | 46 × 34 | No | [98] | 2008 |
| 908 – 914 | -60 | — | -3 | — | — | — | Yes | [100] | 2008 |
| 908 – 914 | -60 | — | -15 | — | — | 50 × 12 | No | [99] | 2008 |
| 865 – 869 | — | — | — | 20 | 15 | 100 × 100 | Yes | [VI] | 2005/2008 |

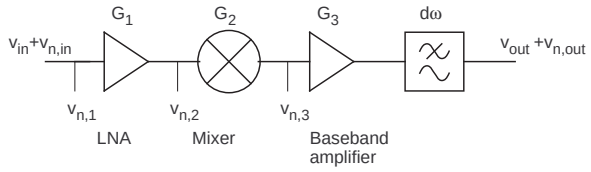


*Figure 4.3. Block diagram of a cascade receiver.*

Similar structures have later been patented also by others [103]. Both [VI] and [VII] analyse noise due to the tunable impedance and the tuner in greater detail than any of the other publications discussed here.

In this chapter, the dynamic range of an RFID reader is analysed. Three isolation techniques are considered: a circulator, a directional coupler, and an adaptive front end as described in [VI]. The adaptive impedance bridge described in [VII] will then be discussed in the context of a mobile reader, where additional design limitations in power consumption and size exist.

## 4.2 Dynamic Range

The dynamic range of a receiver describes the highest and the lowest signal that can be inserted into the receiver, so that the data can still be successfully detected. At low-power, the limiting factor is the noise of the receiver. This is described by the receiver sensitivity $S$. At high-power, the receiver saturation deteriorates the receiver functionality. Saturation is described by input compression point $P_{1dB}$. The dynamic range is the ratio of the input compression point and the input sensitivity.

*Receiver Sensitivity*

To compare the receiver noise with the incoming signal, the concept of input-referred noise is used. It is illustrated in Fig. 4.3. The receiver consists of a low-noise amplifier (LNA), a mixer, and a baseband amplifier, which all add their noise to the signal. The noise is white and is modelled as as input referred noise source with spectral density $v_n$. Every stage also has its gain $G$ (or loss in case of diode ring mixers). The signal at the output is $v_{out} = G_1G_2G_3v_{in}$ and the noise spectral density is $v_{n,out} = G_3(v_{n,3} + G_2[v_{n,2} + G_1\{v_{n,1} + v_{n,in}\}])$. The noise is referred to the input by dividing with the cascade gain, i.e. $v_{n,ref} = v_{n,out}/(G_1G_2G_3)$. The input-

referred noise $v_{n,ref}$ takes into account the noises of the latter stages, and it can be compared directly to the incident signal.

If one calculates the signal-to-noise ratios (SNR) at input and baseband output, one gets

$$\begin{aligned} \frac{SNR_{in}}{SNR_{out}} &= 1 + v_{n,1}/v_{n,in} + \frac{v_{n,2}/v_{n,in}}{G_1} + \frac{v_{n,3}/v_{n,in}}{G_1 G_2} \\ &= F_1 + \frac{F_2 - 1}{G_1} + \frac{F_3 - 1}{G_1 G_2}, \end{aligned} \tag{4.1}$$

which is the well-known equation for the noise figure $F$ of a cascade system [104].

To determine the receiver sensitivity, i.e. the weakest signal to be detected, we have to limit the noise bandwidth $df$ of the receiver. The overall input-referred noise power $S$ is an integral of the noise voltage spectral density divided by the impedance level $R$ of the receiver.

$$S = \frac{1}{R} \int_0^\infty |v_{n,ref}(f)|^2 df. \tag{4.2}$$

This is also called the sensitivity of the receiver. Here the sensitivity is defined for the signal-to-noise ratio being SNR = 1. The sensitivity can also be defined by referring to some value of the bit error ratio (BER), as seen in the reader review in Table 2.2. Usually an SNR>10 dB is required for a reasonably low bit error ratio (BER) [46, 58].

*Input Compression*

The receiver has a gain that is usually measured with a small incoming signal. However, if the signal power is increased, at some power level, the receiver will saturate, i.e. the gain begins to diminish. The output power of RF devices is limited. When the limit is reached, the device cannot drive more power to the load impedance. The saturation causes not only diminishing gain, but also distortion.

Saturation can be described by several parameters, such as the third-order intercept point $IP3$, which is based on the amount of harmonics generated, or the 1 dB compression point $P_{1dB}$, which is based on the gain compression. In this context we use the 1 dB input compression point, which is defined as the input power $P_{in}$ that causes the receiver gain to diminish by 1 dB. The definition is clarified by Fig. 4.4. The input compression point is a convenient measure for the saturation, because it is easy

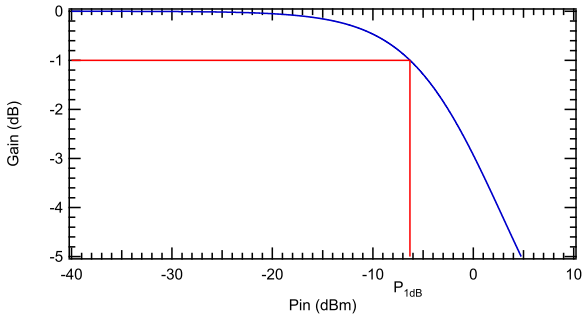


*Figure 4.4. Definition of the input compression point $P_{1dB}$. The gain of the receiver drops by 1 dB at the input power $P_{1dB}$.*

to measure. In the context of RFID, the input compression is caused by the carrier signal at $f_0$, not the information carrying sidebands, which carry very low power. Thus we have $P_{in} \approx P_{in}(f = f_0)$.

The generation of harmonics also introduces third order mixing products that can diminish the signal significantly. In [46], it is shown that at certain phase and amplitude values of the incoming carrier signal, the third order mixing products can cancel the signal altogether. This would be seen in Fig. 4.4 as a deep notch at the gain slope.

## 4.3 Reader with Common Isolation Techniques

In [VI] an RFID reader with an adaptive RF front end is presented. The reader design enables comparing a bistatic common reader with a one having an adaptive RF front end, because the adaptive front end can be shut down. This is called the *open loop* case in [VI], because the feedback loop is opened. The *closed loop* case describes the adaptive RF front end. The photograph of the circuitry is presented in Fig. 4.5.

*Sensitivity*

A block diagram of a bistatic RFID reader is presented in Fig. 4.6. The dynamic range analysis presented here is valid for a circulator and a directional coupler, too. In phasor notation, the local oscillator voltage signal is of the form $V_{LO} = (A + \delta A)\exp(j\omega_0 t + j\delta\varphi)$, where the amplitude and phase noises are denoted by $\delta A$ and $\delta\varphi$, respectively. The power amplifier has complex gain $G_{TX}$. In practice the power amplifier adds white noise

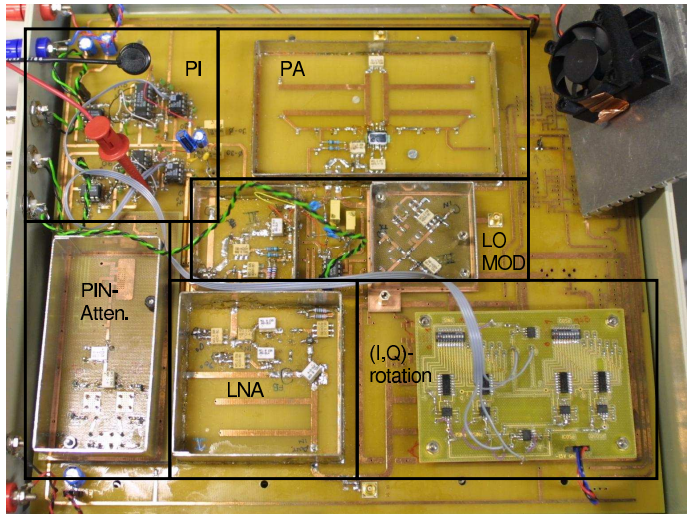


*Figure 4.5. Photograph of the RFID reader circuitry presented in [VI].*

to the signal, but this can be neglected, because phase noise dominates it by tens of decibels. Now the transmitted signal can be written as

$$V_{TX} = G_{TX}(A + \delta A)\exp(j\omega_0 t + j\delta\varphi). \tag{4.3}$$

The transmitted signal couples to the receiver with a complex coupling $L_{TX/RX}$. The coupling arises from reader architecture and environment. The magnitude of the coupling has been estimated for various architectures in [41]. In bistatic systems coupling of -30 dB is typical, and for monostatic systems a coupling of -20 dB is to be expected. The coupling is actually limited by the antenna return loss.

The transponder modulates the transmitted CW signal with data that we assume to be sinusoidal at frequency $\omega_{mod}$ and noiseless, for simplicity. Hence, the signal incident on the receiver is

$$\begin{aligned} V_{RX} &= L_{TX/RX}G_{TX}(A + \delta A)\exp(j\omega_0 t + j\delta\varphi) \\ &+ L_{path}(A + \delta A)\exp(j[\omega_0 + \omega_{mod}]t + j\delta\varphi), \end{aligned} \tag{4.4}$$

where $L_{path}$ is the complex attenuation of the radio path (reader-tag-reader).

The receiver gain is $G_{RX}$ and the noise of the whole cascade receiver is described by its input-referred noise voltage $v_{n,ref}$. The signal is then

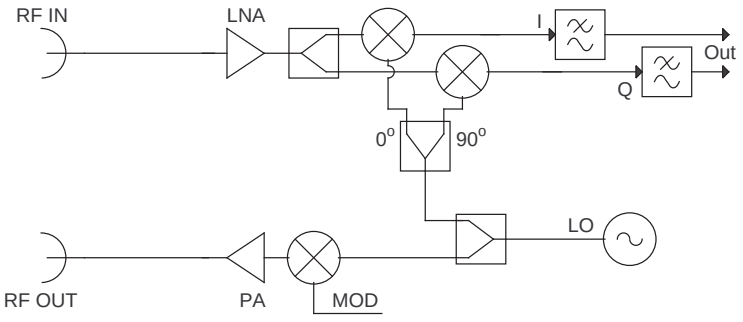


*Figure 4.6. Block diagram of a bistatic common reader configuration.*

detected by a mixer (conversion loss included in the receiver gain) using the same local oscillator that was used for $tx$. Because the radio path is short compared with the modulation wavelength, the phase and amplitude noises correlate, eliminating the phase noise [94]. The amplitude noise is amplified by the correlation, but the use of a balanced mixer suppresses it by tens of decibels (term $L_A$). Hence the baseband signal is of the form

$$\begin{aligned} V_{BB} &= G_{RX} L_{TX/RX} G_{TX} (A^2 + 2 L_A A \delta A) \\ &+ G_{RX} n_{ref} + G_{RX} L_{path} G_{TX} A^2 \exp(j\omega_{mod} t), \end{aligned} \tag{4.5}$$

where the amplitude noise term at the modulation frequency is omitted, because we have $L_A L_{path} \ll 1$.

The first term in Eq. (4.5) describes a DC voltage that is proportional to the incident carrier power. As the coupling coefficient $L_{TX/RX}$ also has a definite phase, mixing the signal down in two orthogonal phases, as shown in Fig. 4.6, gives a complete description of the incident carrier amplitude and phase. The second term is an amplitude noise term that is proportional to the incident carrier power. The third term describes the white noise, i.e. the noise figure of the receiver. The fourth term is the signal from the transponder.

The noise can be referred to the input to give an expression for the sensitivity [VI]

$$S = S_{RX} + \alpha_O P_{in}. \tag{4.6}$$

Here, the term $S_{RX}$ describes the white noise of the receiver. The latter term is due to the transmitter noise and is proportional to the incident carrier power.

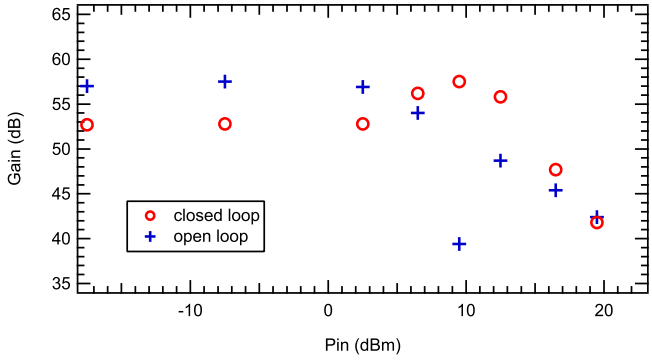


*Figure 4.7. Measured gain from RF input single sideband to baseband output at 20 kHz offset from the carrier as a function of the incident carrier power. Signal power is kept constant throughout the measurement and only the carrier power is altered [VI].*

*Input Compression*

In the reader shown in Fig. 4.6, the input compression is limited by the low-noise amplifier (LNA) or the mixer. The compression points of the devices depend greatly on the technology they are fabricated with.

The prototype described in [VI] has a diode ring mixer (Mini-Circuits JMS-2LH) with $P_{1dB} \approx 5$ dBm , and LNA (Mini-Circuits MAV-11SM) with $P_{1dB} \approx 7$ dBm. The input compression is determined by the mixer, and it should be ca. -5 dBm.

The measurement of the open loop case shown in Figs. 4.7 and 4.8 describes the common reader. The input compression point and the reader sensitivity are $P_{1dB} \approx +4$ dBm and $s \approx -160$ dBm/Hz, respectively. There is additional attenuation due to the filters and the coupler circuits before the LNA. Figure 4.8 also clearly shows the effect of the carrier-induced amplitude noise term, which raises the sensitivity above $P_{in}$ = -5 dBm.

In the worst case, the incident carrier power can be up to +10 dBm. Hence, the compression point has to be raised. The simplest way to do this would be to add attenuation before the LNA, or replace the circulator with a directional coupler in the case of a monostatic reader. This deteriorates the sensitivity. The noise of the latter stages has a higher impact, and the sensitivity will rise more than just by the amount of the added attenuation. The compression point, on the other hand, rises only by the amount of the attenuation.

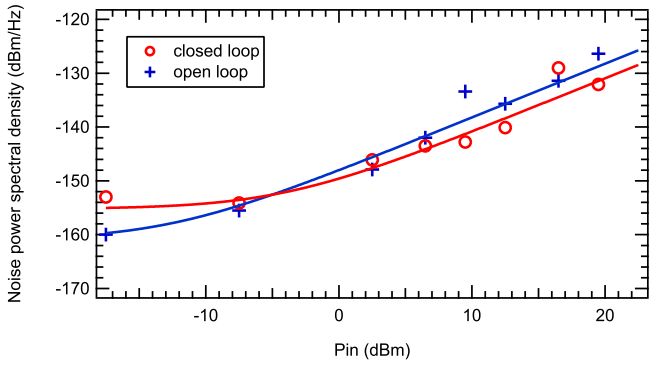


*Figure 4.8. Measured input-referred noise at 50 kHz offset from the carrier as a function of the incident carrier power [VI].*

The attenuator significantly decreases the signal-to-noise ratio at low incident carrier power, when the receiver white noise is the dominant noise mechanism. However, because the attenuator affects equally to the signal and carrier induced noises, the signal-to-noise ratio is not affected at high incident carrier power, when the carrier-induced noise is dominant. However, the higher white noise is the dominant noise mechanism at higher incident power levels.

## 4.4 Adaptive RF Front End

*Feedback Principle*

Another approach to dynamic range improvement is the use of feedback. The DC component of the mixer output signal describes the incident carrier amplitude and phase, and this signal can be used as an input for an adaptive RF isolator circuit. The feedback is described in [VII], and the block diagram of the front end with feedback is presented in Fig. 4.9.

The basic idea of the circuit is to add a compensation signal of equal magnitude and opposite phase to the incident signal. The feedback signal $c_F$ can be calculated by equating it with the open loop feedback signal $c_{FO}$. The signal incident on the LNA becomes

$$c_F + c_R = c_R \frac{1}{1 - c_D^* c_D G\left(\omega_R - \omega_0\right)}, \tag{4.7}$$

where $c_D$ describes the phase shift in the loop. To eliminate the coupling from the receiver, but to let the signal from the transponder pass

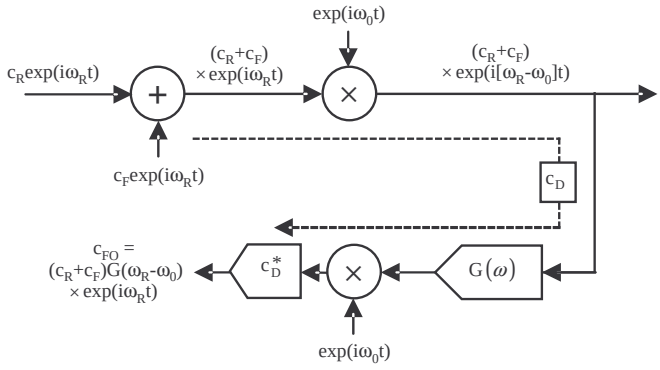


*Figure 4.9. Signal flow of the quadrature feedback in the case of complex-valued signals [VI].*

unhindered, the loop gain is selected to be of low-pass type with a cut-off frequency well below the data band, i.e. $G(\omega) = -G_0/(1 + i\omega/\omega_C)$. Additionally, a perfect phase compensation is assumed. Now the signal incident on the LNA is

$$c_R + c_F = c_R \left(1 + G_0 \frac{\omega_C}{\omega_C + i\,(\omega_R - \omega_0)}\right)^{-1}. \tag{4.8}$$

Below the cut-off frequency, the feedback suppresses all signals by $(1+G_0)$, and above the cut-off the signals are not affected.

*Sensitivity*

In Fig. 4.10, a bistatic reader with an adaptive RF front end is shown. The circuit is described in [VI]. The reader utilises quadrature feedback for carrier suppression. The idea has earlier been exploited in frequency modulated continuous wave (FMCW) radars, where the receiver exhibits similar carrier coupling from the reader [105, 106].

The sensitivity analysis begins with the incident signal, which is identical to the traditional reader (see Eq. (4.4)). A compensation signal of the form

$$V_{FB} = (C + \delta C)(A + \delta A)\exp(j\omega_0 t + j\delta\varphi) + n_{FB} \tag{4.9}$$

is added to the incident signal. The compensation signal carries the same noise as the incident signal, but also new noise terms from the baseband loop amplifiers, i.e. white noise $n_{FB}$ and non-white amplitude noise $\delta C$,

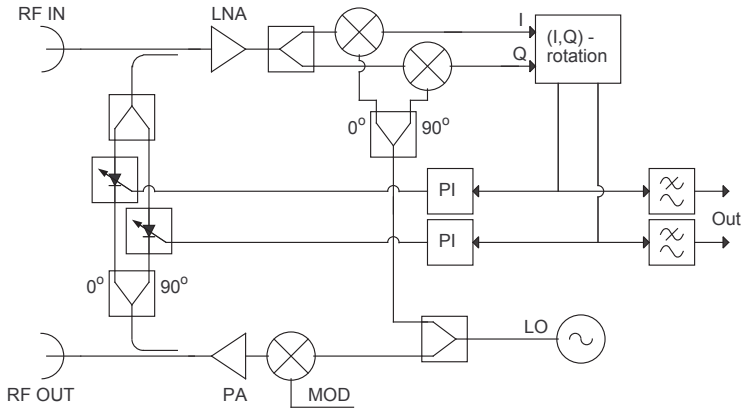


*Figure 4.10. Block diagram of a bistatic reader with an adaptive RF front end [VI].*

which can arise, e.g. from leakage of the carrier-induced amplitude noise through the loop.

When the feedback is closed, according to Eq. (4.7), the signal incident on the LNA is suppressed at the feedback band by $(1+G_0)$. With high gain, i.e. $G_0 \gg 1$, the compensation signal is equal in magnitude and opposite in phase compared with the incident carrier signal, giving

$$C = -L_{TX/RX} G_{TX} A. \tag{4.10}$$

The incoming carrier and the compensation signal carry correlated amplitude noise $\delta A$ with them. The noise is correlated within the feedback and data bands due to range correlation [94]. Hence, when suppressing the carrier at the feedback band, the amplitude noise is suppressed also at the data band by the factor $(1 + G_0)$.

The feedback will introduce its own noise sources to the system. The feedback signal will emit at least white noise $n_{FB}$ due to thermal sources. Also, the amplitude term cannot be assumed to be completely filtered by the loop gain. The noncorrelated amplitude noise term $\delta C$ may arise for example from amplitude-noise leakage from the downmixer, or from PIN-diode shot noise. These noise components do not affect the feedback, and can be directly added to the signal.

The signal incident to the LNA can now be written as

$$\begin{aligned} V_{RX} + V_{FB} &= \frac{1}{1+G_0} L_{TX/RX} G_{TX} (A + \delta A) \exp(j\omega_0 t + j\delta\varphi) \\ &+ A(C\frac{\delta C}{C} + n_{FB}) \\ &+ L_{path}(A + \delta A) \exp(j[\omega_0 + \omega_{mod}]t + j\delta\varphi). \end{aligned} \tag{4.11}$$

Here the first and second terms describe the incident carrier and its amplitude noise, respectively. These are suppressed by the loop feedback band gain also at the data band due to signal correlation. The third term is the amplitude noise introduced by the feedback loop. It has been emphasised that the amplitude noise term $\delta C$ is dependent on the compensation signal voltage $C$, i.e. on the incident carrier power. The fourth term is the white noise of the baseband amplifiers and the last term is the signal from the transponder.

Again, the phase noise is correlated and suppressed in the downmixer. Hence, in the case of high loop gain ($G_0 \gg 1$), the baseband signal becomes

$$\begin{aligned} V_{BB} &= \frac{1}{G_0} L_{TX/RX} G_{TX} (A^2 + 2AL_A \delta A) \\ &+ L_{TX/RX} G_{TX} A^2 \frac{\delta C}{C} + A^2 n_{FB} \\ &+ L_{path} A^2 \exp(j\omega_{mod} t), \end{aligned} \tag{4.12}$$

where we have used the feedback criterion $C = -L_{TX/RX} G_{TX} A$. In terms of power, the receiver sensitivity is [VI]

$$S = S_{RX} + S_F + \frac{\alpha_O P_{in}}{G_0} + \alpha_F P_{in}. \tag{4.13}$$

The carrier amplitude noise is suppressed by the loop gain, but additional white and amplitude-dependent terms arise. In practice this means, that sensitivity at low incident power is somewhat higher because of the feedback white noise $S_F$, but at higher incident power, the sensitivity can be better than without the feedback, if $\alpha_F < \alpha_O$.

*Input Compression*

The linearity is limited by the feedback loop. The criteria in Eq. (4.7) and the subsequent reasoning hold as long as the feedback loop can drive sufficient power to the input of the LNA. Hence, the compression is defined

by the active component in the feedback loop. A PIN diode attenuator similar to that in [107] is an optimum choice here, because it can handle high power up to 20 dBm, and still have basically thermally limited noise characteristics. Use of a diode ring mixer easily limits the output power to about 0 dBm, which falls short by 10 dB. Adding an amplifier after the mixer in the feedback loop increases $S_F$ by the gain of the amplifier, making it an infeasible solution. Both the sensitivity and the linearity, i.e. the dynamic range of the receiver, are determined by the upmixer component in the feedback loop [VI].

The sensitivity and compression point of a realised adaptive front end in [VI] can be seen in Figs. 4.7 and 4.8. The front end is measured with the feedback loop both closed and open, giving a comparison between a traditional reader with LNA and an adaptive front end. It is seen that the feedback increases the white noise level by almost 10 dB, but noise suppression leads to a smaller noise term due to the incident carrier. At the same time, the input compression point of the receiver is increased by more than 10 dB.

## 4.5 Impedance Bridge as an Adaptive RF Front End

In hand-held devices, there are three main design objectives. The devices must be small in size and power consumption, and it has to be mass producible with low cost. Hence physically small antennas have to be used in hand-held devices. The small antennas tend to be narrow-banded in nature and sensitive to near-field effects, e.g. dielectric loading by the user hand. The mobile RFID reader has generated several small antenna designs [108, 109, 110]. The mobile phone manufacturers have been developing RFID readers. In [58], an integrated UHF RFID reader IC described by Samsung, and a prototype of a mobile phone with an embedded RFID reader is presented in [111] by Nokia.

In addition to delivering isolation and high dynamic range, the adaptive RF front end can be used to tune the reader antenna to the operating frequency, despite the user hand. This optimises the impedance matching between the power amplifier (PA) and the antenna, enabling a high read range with low power consumption.

In [VII] an adaptive front end with a four-port isolator is described. The block diagram and the circuit model of the reader RF front end are

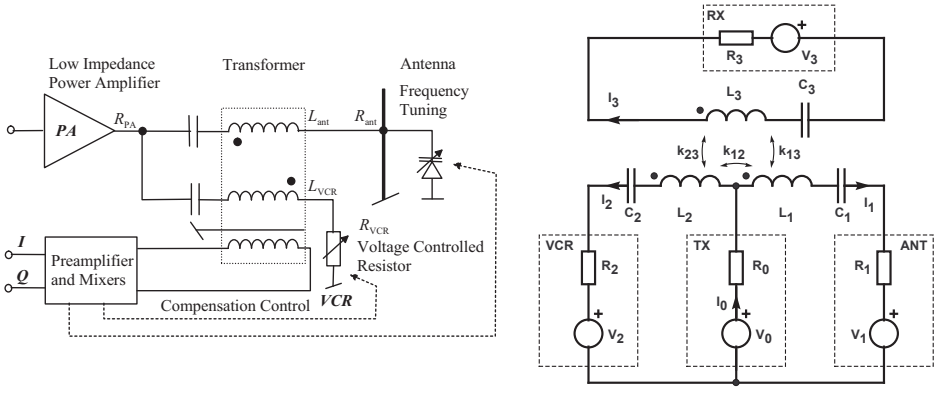


*Figure 4.11. Block diagram (left) and circuit model (right) of an impedance bridge as an adaptive front end [VII].*

presented in Fig. 4.11 and a photograph of the prototype in Fig. 4.12. The isolator is realised as a hybrid transformer with unequal coupling between the antenna and voltage controlled resistor (VCR) ports. Hence, the device could be described as a directional coupler. The directional coupler adds attenuation to the $rx$ path, compromising the sensitivity of the receiver. However, in situations, where the backscattered signal is relatively high, i.e. the operating range is short, the solution is feasible. This is the case with a hand-held reader, which usually transmits a lower power (100 – 500 mW) to save battery.

The bridge enables increasing the compression point in the same manner than with the adaptive front end described in [VI], but with less components. Only a transformer, a PIN diode and a varactor, instead of two directional couplers, two PIN diode attenuators and two power dividers are needed. Hence, the transformer-based solution is better for size-critical applications, e.g. hand-held devices.

The bridge can be thoroughly analysed by writing the network equations of the circuit model presented in Fig. 4.11. The operation principle is simple. The antenna is tuned to resonance by the varactor. The branches of the bridge are also in resonance, i.e. $L_1$ resonates with $C_1$, as well as $L_2$ with $C_2$. Isolation is achieved by tuning the VCR resistance to

$$\frac{R_1}{R_2} = \frac{M_{13}}{M_{23}} = \frac{k_{13}}{k_{23}}\sqrt{\frac{L_1}{L_2}}. \tag{4.14}$$

A measurement of the prototype described in [VII] is shown in Fig. 4.13, with the isolation and $rx$ and $tx$ gains given as a function of frequency.

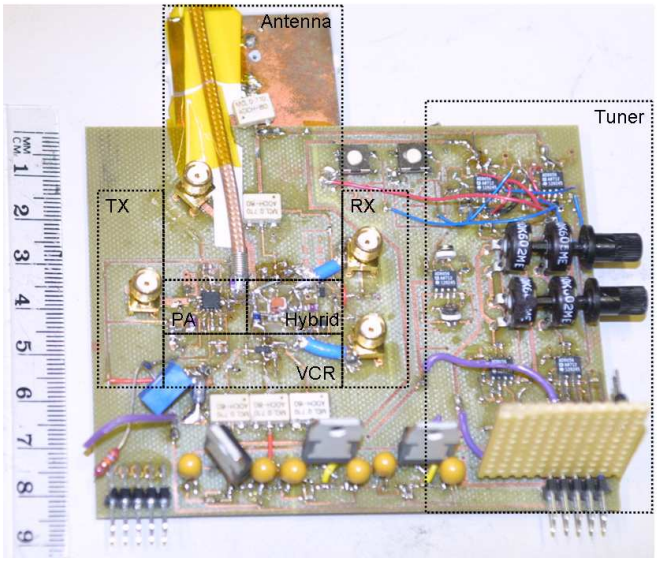


*Figure 4.12. Photograph of the impedance bridge prototype [VII].*

The power dissipated in the loads $R_1$ and $R_2$ depends only on the resistances according to

$$\frac{P_1}{P_2} = \frac{R_2}{R_1} = n, \tag{4.15}$$

which defines the power ratio $n$. Because inductance of a wire wound coil is proportional to the square of the turns of wire in the coil, the power ratio $n$ describes also the ratio of turns in coils $L_1$ and $L_2$ (see Eq. 4.14). Hence the hybrid transformer can be designed for any power ratio between the loads. The power ratio $n$ also affects the gain in $tx$ and $rx$ paths, $G_{TX}$ and $G_{RX}$ respectively, and hence the noise figure $F$ of the bridge as a receiver. Theoretical results can be summarised as [VII]

$$\begin{aligned} G_{TX} &= \left(1 + \frac{1}{n}\right)^{-1}, \\ G_{RX} &\propto \frac{1}{n^2}, \\ F &\propto n^3. \end{aligned} \tag{4.16}$$

For power saving, i.e. for achieving low transmission loss, a high value of $n$ would be preferable, but the noise figure increases fast with increasing $n$.

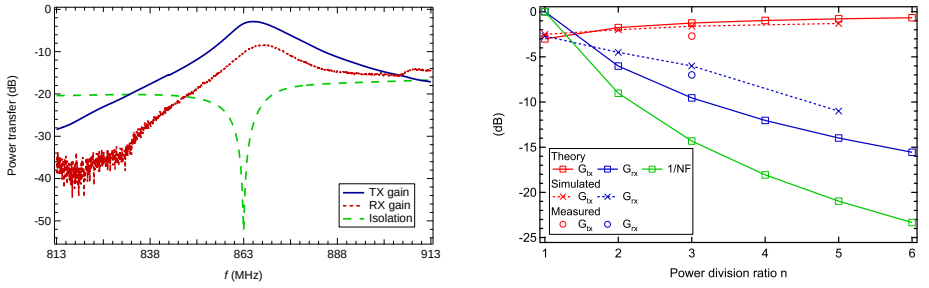


*Figure 4.13. Measured results of isolation and tx and rx gains of the bridge as a function of frequency (left), and transmission and reception gains ($G_{TX}$ and $G_{RX}$), and the noise figure $F$ of the bridge at isolation frequency as a function of the power ratio n (right) [VII].*

Thus a compromise has to be found. The compromise taken in [VII] is n≈3. The analytical results of Eq. (4.16), simulations of the bridge and measurement results are summarised in Fig. 4.13. The figure shows that the measurements are in good agreement with the theory and simulations.

## 4.6 Summary

In this chapter, RFID readers with three different isolation techniques have been discussed, i.e. the common reader with a bistatic configuration (or a circulator), a common reader with a directional coupler, and a reader with an adaptive RF front end. The design and development of two adaptive RF front ends was presented: a full power (0.5 $W_{erp}$) reader in [VI] and a lower power reader for mobile applications in [VII]. The sensitivity and compression point of the readers was analysed and measured, and they were compared to other published isolation techniques and readers.

The dynamic range of the different reader architectures is summarised here. Typical values of sensitivity and input compression point of the readers are schematically presented in Fig. 4.14. The values are based on the measurements in [VI], except for the geometry with directional coupler, which has been calculated based on the measurement results of the bistatic reader and the measurement results of the attenuation of the impedance bridge in [VII]. Using a directional coupler is equal to adding attenuation in front of the receiver of the bistatic reader.

The attenuation at the receiver can be used to rise the input compression

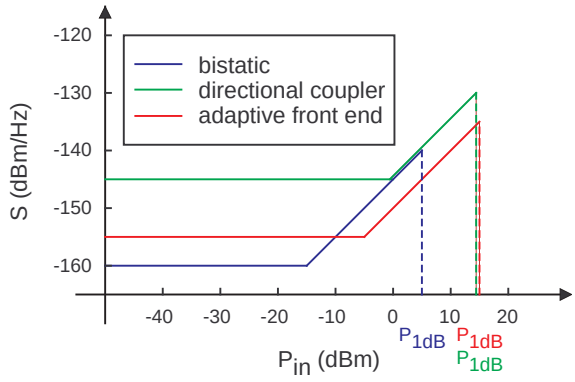


*Figure 4.14. Typical sensitivity $S$ and input compression point $P_{1dB}$ of different reader architectures as a function of the incident carrier power $P_{in}$.*

point, but it also diminishes the dynamic range: Sensitivity is increased more than the compression point due to the noise contribution of latter stages. The impedance bridge used in [VII] is similar to the directional coupler, but the adaptivity enables small size and low power consumption, which are essential in mobile devices.

At best, the dynamic range of the published readers is comparable to that of a the bistatic reader (see Table 2.2). Hence, the adaptive front end presented in [VI] has supreme dynamic range.

# 5 Conclusion

In this Thesis, RF components and phenomena in passive UHF RFID systems were studied. The basic equations for transponder powering and backscattering communication were derived. The analysis was applied to RFID at UHF and millimetre waves. The read range of passive UHF RFID is limited by the power transfer to the transponder, provided that the sensitivity of the reader is not compromised by the coupling from the transmitter. To ensure this, high isolation between the transmitter and the receiver of the reader is required. The sensitivity of the transponders is improving with the introduction of semipassive transponders. The more sensitive the transponders become, the more important the reader sensitivity will be.

In the Thesis, the dynamic range of the RFID reader was analysed in detail, and the development of two RFID readers with adaptive RF front ends was presented. The sensitivity and compression point of the readers was analysed and measured and compared to other readers published in literature. The reader with adaptive front end presented in [VI] has the highest dynamic range among them all. It combines low noise characteristics and high input compression, enabling longer range RFID systems.

The UHF RFID is applied in logistics and in retail industry for tracking ever smaller pallets and boxes, and recently even item level tagging has been introduced. Hence, even consumers could begin to use handheld readers to access further information on the merchandise. Mobile phone manufacturers have already shown interest for integrating an UHF RFID reader into mobile phones [111], even though the devices are not yet rolled out to the general public. A reader in a small mobile phone is very prone to disturbances caused by the user hand and other objects in the imminent near environment of the reader antenna. An adaptive RF front end, such as the one presented in [VII], is needed for efficient and reliable operation.

The adoption of RFID in new applications and environments demands also suitable transponder antennas. Tagging of an item cannot be economically feasible, if placing the transponder on an item requires an RF

specialist, or if a transponder antenna has to be specially developed for every different item. Even though an ultimate universal transponder, fitting every application, is a day-dream, research on platform-tolerant antennas has already lead to several designs, such as the one introduced in [III]. The development has been rapid in the recent years. First universal transponders emerged less than five years ago, and nowadays there are at least a dozen companies selling their designs. However, most of the universal transponders are expensive, costing tens of times as much as the 10 cent labels. Hence, the design of a specialised low cost antenna is still feasible for tagging mass products.

In the future, passive sensor nodes, like the one introduced in [I], could be utilised to measure room temperature, moisture, pressure in tires, etc. And the consumer could access the node with the reader in his/her cell phone. Another future development in the field of RFID will propably be the adoption of higher carrier frequencies in the microwave and millimetre wave ranges. The higher carrier frequency does not affect the operating principles of RFID, but it will modify the compromise between power transfer and backscattering modulation. The millimetre RFID, or millimetre wave identification (MMID), was analysed in [II]. Power transfer at millimetre waves is not feasible, but semipassive systems could provide features impossible to implement with UHF. At millimetre waves, data bandwidth of hundreds of megabits could be implemented. A reader antenna with narrow beam could be used to select a single transponder in a swarm of nearby transponders. Finally, the existing automotive radars have all the hardware needed to communicate with MMID transponders.

The field of RFID and backscattering communication has been studied for 60 years. A set of applications has reached maturity, but the field has not found its limits yet. The power efficiency and simple implementation of the backscattering modulation promise new applications in the future.

# References

[1] RFID Journal, "Wal-Mart Tackles Out-of-Stocks", April 2005, www.rfidjournal.com/article/articleview/1551/1/1/, referenced September 5th 2008.

[2] K. Finkenzeller, *RFID Handbook*, 2nd edition, John Wiley & Sons, 2003.

[3] RFIDJournal, "Stealing Cars Will Get Tougher", July 2002, www.rfidjournal.com/article/articleview/33/1/1/, referenced September 14th 2008.

[4] RFIDJournal, "Passive Tags Track Cars", August 2004, www.rfidjournal.com/article/articleview/1078/1/1/, referenced September 14th 2008.

[5] RFIDJournal, "UHF Tags Enter the Timing Race", October 2007, www.rfidjournal.com/article/articleview/3691/1/1/, referenced September 4th 2008.

[6] RFID Gazette, "RFID Implants: 5 Amazing Stories", April 2007, www.rfidgazette.org/2007/04/rfid_implants_5.html, referenced September 4th 2008.

[7] Ekhau Inc., "Madrid Hospital Improves Employee Safety with Ekahau Wi-Fi RTLS", press release, June 2008, www.ekahau.com/?id=20089, referenced September 4th 2008.

[8] Nokia 6131 NFC, www.nokia.com, referenced September 5th 2008.

[9] C. S. Hartmann and L. T. Claiborne, "Fundamental Limitations on Reading Range of Passive IC-Based RFID and SAW-Based RFID", *IEEE International Conference on RFID*, Grapevine, Texas, USA, March 26 – 28, 2007, pp. 41 – 48.

[10] P. V. Nikitin, S. Lam, and K. V. S. Rao, "Low Cost Silver Ink RFID Tag Antennas", *IEEE Antennas and Propagation Society International Symposium*, Vol. 2B, July 3 – 8, 2005, pp. 353 – 356.

[11] V. Subramanian, J. M. J. Frchet, P. C. Chang, D. C. Huang, J. B. Lee, S. E. Molesa, A. R. Murphy, D. R. Redinger, and S. K. Volkman, "Progress Toward Development of All-Printed RFID Tags: Materials, Processes, and Devices", *Proceedings of IEEE*, Vol. 93, No. 7, pp. 1330 – 1338, July 2005.

[12] Kovio Inc., www.kovio.com; RFIDJournal, www.rfidjournal.com/article/articleview/4389/; and www.pennwellblogs.com/sst/eds_threads/2007/11/071123-printed-silicon-rf-ids-by-kovio.php?dcmp=WaferNEWS_ARCH, November 2007 – October 2008, referenced November 31st 2008.

[13] PolyIC GmbH & Co. KG, "The Revolution with Printed Electronics Begins – First Printed RFID and Smart Objects for the Market", press release, September 25, 2007, www.polyic.com/en/read.php?page=306, referenced September 4th 2008.

[14] P. F. Baude, D. A. Ender, T. W. Kelley, M. A. Haase, D. V. Muyres, and S. D. Theiss, "Organic Semiconductor RFID Transponders", *IEEE Electron Devices Meeting, IEDM '03 Technical Digest.*, 2003.

[15] J. C. Maxwell, "A Dynamical Theory of the Electromagnetic Field", *Philosophical Transactions of the Royal Society of London*, 1865.

[16] N. Tesla, "Apparatus for Transmission of Electrical Energy", *US Patent 649621*, May 1900.

[17] N. Tesla, "Art of Transmitting Electrical Energy Through the Natural Mediums", *US Patent 787412*, April 1905.

[18] H. T. Friis, "A Note on a Simple Transmission Formula", *Proceedings of the IRE*, Vol. 34, Issue 5, pp. 254 – 256, May 1946.

[19] W. C. Brown, "The History of Power Transmission by Radio Waves", *IEEE Transactions on Microwave Theory and Technology*, Vol. 32, Issue 9, pp. 1230 – 1242, September 1984.

[20] H. Stockman, "Communication by Means of Reflected Power", *Proceedings of the IRE*, pp. 1196 – 1204, October 1948.

[21] D. D. King, "Measurement and Interpretation of Antenna Scattering", *Proceedings of the IRE*, Vol. 37, pp. 770 – 777, July 1949.

[22] R. F. Harrington, "Theory of Loaded Scatterers", *Proceedings of the IEE*, Vol. 111, pp. 617 – 623, April 1964.

[23] R. F. Harrington, "Field Measurements Using Active Scatterers", *IEEE Transactions on Microwave Theory and Technology*, Vol. 11, p. 454, September 1963.

[24] J. Appel-Hansen, "Accurate Determination of Gain and Radiation Patterns by Radar Cross-Section Measurements", *IEEE Transactions*

*on Antennas and Propagation*, Vol. 27, pp. 640 – 646, September 1979.

[25] J. T. Mayhan, A. R. Dion, and A. J. Simmons, "A Technique for Measuring Antenna Drive Port Impedance Using Backscatter Data", *IEEE Transactions on Antennas and Propagation*, Vol. 42, pp. 526 – 532, April 1994.

[26] W. Wiesbeck and E. Heidrich, "Wide-Band Multiport Antenna Characterization by Polarimetric RCS Measurements", *IEEE Transactions on Antennas and Propagation*, Vol. 46, pp. 341 – 350, March 1998.

[27] "The Great Seal Bug Story", www.spybusters.com/Great_Seal_Bug .html, referenced August 14th 2008.

[28] Wikipedia, http://en.wikipedia.org/wiki/Identification_friend_or_foe; and http://en.wikipedia.org/wiki/Secondary_Surveillance_Radar, referenced August 14th 2008.

[29] A. R. Koelle, S. W. Depp, and R. W. Freyman, "Short-Range Radio-Telemetry for Electronic Identification, Using Modulated RF Backscatter", *Proceedings of the IEEE*, Vol. 63, Issue 8, pp. 1260 – 1261, August 1975.

[30] J. Landt, *Shrouds of Time: The History of RFID*, AIM, 2001, www.transcore.com/pdf/AIM shrouds_of_time.pdf, referenced August 14th 2008.

[31] K. V. S. Rao, "An Overview of Back Scattered Radio Frequency Identification System (RFID)", *IEEE Asia Pacific Microwave Conference*, Vol. 3, 1999, pp. 746 – 749.

[32] The Palomar Project, "Passive Long Distance Multiple Access UHF RFID System", Public Report, European Commission, Project Number IST1999-10339, November 2002.

[33] *ISO/IEC 18000-6: Information Technology — Radio Frequency Identification for Item Management — Part 6: Parameters for Air Interface Communications at 860 MHz to 960 MHz*, www.iso.org, ISO, 2004.

[34] *EPC Radio Frequency Identification Protocols: Class-1 Generation-2 UHF RFID, Protocol for Communications at 860 – 960 MHz, Version 1.1.0.*, www.epcglobalinc.org, EPCglobal, 2006.

[35] The European Telecommunications Standards Institute (ETSI), www.etsi.org.

[36] Federal Communications Commission (FCC), www.fcc.gov.

[37] RFID Journal, "China Approves Requirements for UHF Bandwidth", May 2007, www.rfidjournal.com/article/articleview/3318/, referenced August 14th 2008.

[38] K. V. S. Rao, D.-W. Duan, and H. Heinrich, "On the Read Zone Analysis of Radio Frequency Identification Systems with Transponders Oriented in Arbitrary Directions", *IEEE Asia Pacific Microwave Conference*, Vol. 3, 1999, pp. 758 – 761.

[39] U. Karthaus and M. Fischer, "Fully Integrated Passive UHF RFID Transponder IC with 16.7-$\mu$W Minimum RF Input Power", *IEEE Journal of Solid-State Circuits*, Vol. 38, pp. 1602 – 1608, October 2003.

[40] P. V. Nikitin and K. V. S. Rao, "Performance Limitations of Passive UHF RFID Systems", *IEEE Antennas and Propagation Society International Symposium*, July 9 – 14, 2006, pp. 1011 – 1014.

[41] P. V. Nikitin and K. V. S. Rao, "Antennas and Propagation in UHF RFID Systems", *IEEE International Conference on RFID 2008*, Las Vegas, NV, USA, April 16 – 17, 2008, pp. 277 – 288.

[42] F. Fuschini, C. Piersanti, F. Paolazzi, and G. Falciasecca, "Analytical Approach to the Backscattering from UHF RFID Transponder", *IEEE Antennas and Wireless Propagation Letters*, Vol. 7, pp. 33 – 35, 2008.

[43] J. D. Kraus, *Antennas*, McGraw-Hill, 1950.

[44] K. Kurokawa, "Power Waves and the Scattering Matrix", *IEEE Transactions on Microwave Theory and Techniques*, Vol. MTT-13, No. 3, pp. 194 – 202, March 1965.

[45] P. V. Nikitin, K. V. S. Rao, S. F. Lam, V. Pillai, R. Martinez, and H. Heinrich, "Power Reflection Coefficient Analysis for Complex Impedances in RFID Tag Design", *IEEE Transactions on Microwave Theory and Techniques*, Vol. 53, No. 9, pp. 2721 – 2725, September 2005.

[46] J.-P. Curty, M. Declercq, C. Dehollain, and N. Joehl, *Design and Optimization of Passive UHF RFID Systems*, Springer, 2007.

[47] J. Sondow and E. W. Weisstein, "Riemann Zeta Function", *MathWorld — A Wolfram Web Resource*, available at http://mathworld.wolfram.com/RiemannZetaFunction.html, referenced July 31st 2008.

[48] X. Q. Bao, W. Burkhard, V. V. Varadan, and V. K. Varadan, "SAW Temperature Sensor and Remote Reading System", *IEEE Ultrasonics Symposium*, 1987, pp. 583 – 586.

[49] A. D. DeHennis and K. D. Wise, "A Wireless Microsystem for the Remote Sensing of Pressure, Temperature, and Relative Humidity", *IEEE Journal of Microelectromechanical Systems*, Vol. 14, No. 1, pp. 12 – 22, February 2005.

[50] V. Pillai, H. Heinrich, D. Dieska, P. V. Nikitin, R. Martinez, and K. V. S. Rao, "An Ultra-Low-Power Long Range Battery/Passive RFID Tag for UHF and Microwave Bands With a Current Consumption of 700 nA at 1.5 V", *IEEE Transactions on Circuits And SystemsI: Regular Papers*, Vol. 54, No. 7, pp. 1500 – 1512, July 2007.

[51] N. Cho, S.-J. Song, S. Kim, S. Kim, and H.-J. Yoo,"A 5.1-$\mu$W UHF RFID Tag Chip Integrated with Sensors for Wireless Environmental Monitoring", *Proceedings of ESSCIRC*, September 12 – 16, 2005, pp. 279 – 282.

[52] J.-P. Curty, N. Joehl, C. Dehollain, and M. Declercq, "Remote Powered Addressable UHF RFID Integrated System", *IEEE Journal of Solid-State Circuits*, Vol. 40, pp. 2193 – 2202, November 2005.

[53] F. Kocer and M. P. Flynn, "A New Transponder Architecture with On-Chip ADC for Long-Range Telemetry Applications", *IEEE Journal of Solid-State Circuits*, Vol. 41, No. 5, pp. 1142 – 1148, May 2006.

[54] A. P. Sample, D. J. Yeager, P. S. Powledge, and J. R. Smith, "Design of a Passively-Powered, Programmable Sensing Platform for UHF RFID Systems", *IEEE International Conference on RFID*, Grapevine, Texas, USA, March 26 – 28, 2007, pp. 149 – 156.

[55] H. Nakamoto, D. Yamazaki, T. Yamamoto, H. Kurata, S. Yamada, K. Mukaida, T. Ninomiya, T. Ohkawa, S. Masui, and K. Gotoh, "A Passive UHF RF Identification CMOS Tag IC Using Ferroelectric RAM in 0.35-$\mu$m Technology", *IEEE Journal of Solid-State Circuits*, Vol. 42, No. 1, pp. 101 – 110, January 2007.

[56] Alien Technology, "Alien H3 EPC Class 1 Gen 2 RFID Tag IC, Product Overview", April 2008, www.alientechnology.com/docs/products/DS_H3.pdf, referenced July 2008.

[57] I. Kipnis, S. Chiu, M. Loyer, J. Carrigan, J. Rapp, P. Johansson, D. Westberg, and J. Johansson, "A 900MHz UHF RFID Reader Transceiver IC", *IEEE International Solid-State Circuit Conference*, February 13, 2007, pp. 214 – 215, 598.

[58] I. Kwon, Y. Eo, H. Bang, K. Choi, S. Jeon, S. Jung, D. Lee, and H. Lee, "A Single-Chip CMOS Transceiver for UHF Mobile RFID Reader", *IEEE Journal of Solid-State Circuits*, Vol. 43, No. 3, pp. 729 – 738, March 2008.

[59] AS3990 Preliminary Datasheet, Austria Microsystems corporation, www.austriamicrosystems.com/03products/products_detail/AS3990/download/AS3990_Features.pdf, referenced August 8th 2008.

[60] Elektrobit Company, "EB RFID Reader EB URP1000-ETSI Datasheet", www.elektrobit.com/file.php?110, referenced May 2008.

[61] D. Neculoiu, G. Konstantinidis, T. Vähä-Heikkilä, A. Müller, D. Vasilache, A. Stavinidris, L. Bary, M. Dragoman, I. Petrini, C. Buiculescu, Z. Hazoupulos, N. Kornilios, P. Pursula, R. Plana, and D. Dascalu, "GaAs Membrane-Supported 60 GHz Receiver with Yagi-Uda Antenna", *MEMSWAVE 2007, 8th International Symposium on RF MEMS and RF Microsystems*, Barcelona, Spain, June 26 – 29, 2007, pp. 15 – 18.

[62] E. M. Biebl,"RF Systems Based on Active Integrated Antennas", *(AEÜ) International Journal of Electronics and Communications*, Vol. 57, No. 3, pp. 173 – 180, 2003.

[63] A. Müller, D. Neculoiu, P. Pursula, T. Vähä-Heikkilä, F. Giacomozzi, and J. Tuovinen, "Hybrid Integrated Micromachined Receiver for 77 GHz Millimeter Wave Identification Systems", *37th European Microwave Conference 2007*, Munich, Germany, October 2007, pp. 1034 – 1037.

[64] D. Kim, M. A. Ingram, and W. W. Smith Jr., "Measurements of Small-Scale Fading and Path Loss for Long Range RF Tags", *IEEE Transactions on Antennas and Propagation*, Vol. 51, No. 8, pp. 1740 – 1749, August 2003.

[65] E. F. Knott, J. F. Schaeffer, and M. T. Tuley, *Radar Cross Section*, Artech House, 1993.

[66] E. Newman and D. Forrai, "Scattering from a Microstrip Patch", *IEEE Transactions on Antennas and Propagation*, Vol. 35, pp. 245 – 251, March 1987.

[67] R. E. Collin, "Limitations of the Thevenin and Norton Equivalent Circuits for a Receiving Antenna", *IEEE Antennas and Propagation Magazine*, Vol. 45, Issue 2, pp. 119 – 124, April 2003.

[68] P. V. Nikitin, K. V. S. Rao, and R. D. Martinez, "Differential RCS of RFID Tag", *IEE Electronic Letters*, Vol. 43, No. 8, pp. 431 – 432, April 2007.

[69] P. V. Nikitin and K. V. S. Rao, "Theory and Measurement of Backscattering from RFID Tags", *IEEE Antennas and Propagation Magazine*, Vol. 48, pp. 212 – 218, December 2006.

[70] M. Ritamäki, A. Ruhanen, V. Kukko, J. Miettinen, and L. H. Turner, "Contactless Radiation Pattern Measurement Method for UHF RFID Transponders", *IEE Electronic Letters*, Vol. 41, Issue 13, pp. 723 – 724, June 2005.

[71] Tagformance Lite, Voyantic Ltd, www.voyantic.com/index.php?trg =browse&id=64, referenced August 14th 2008.

[72] P. Pursula, T. Varpula, K. Jaakkola, and M. Hirvonen, "Antenna Radiation Characterization by Backscattering Modulation", *Proceedings of URSI/IEEE XXIX Convention on Radio Science*, Espoo, Finland, November 1 – 2, 2004, pp. 115 – 118.

[73] S.-J. Kim, B. Yu, Y.-S. Chung, F. J. Harackiewicz, and B. Lee, "Patch-Type Radio Frequency Identification Tag Antenna Mountable on Metallic Platforms, *Microwave and Optical Technology Letters*, Vol. 48, No. 12, pp. 2446 – 2448, December 2006.

[74] B. Yu, S.-J. Kim, B. Jung, F. J. Harackiewicz, and B. Lee, "RFID Tag Antenna Using Two-Shorted Microstrip Patches Mountable on Metallic Objects", *Microwave and Optical Technology Letters*, Vol. 49, Issue 2, pp. 414 – 416, February 2007.

[75] B. Lee and B. Yu, "Compact Structure of UHF Band RFID Tag Antenna Mountable on Metallic Objects", *Microwave and Optical Technology Letters*, Vol. 50, Issue 1, pp. 232 – 234, January 2008.

[76] C. Icheln, "The Construction and Application of a GTEM cell", *Master's Thesis*, Technical University of Hamburg, Hamburg, Faculty of Electrical Engineering and Helsinki University of Technology, Faculty of Electrical Engineering, November 1995.

[77] K. V. S. Rao, P. V. Nikitin, and S. F. Lam, "Antenna Design for UHF RFID Tags: A Review and a Practical Application", *IEEE Transactions on Antennas and Propagation*, Vol. 53, No. 12, pp. 3870 – 3876, December 2005.

[78] L. J. Chu, "Physical Limitations of Omni-Directional Antennas", *Journal of Applied Physics*, Vol. 19, pp. 1163 – 1175, December 1948.

[79] R. E. Collin and S. Rothchild, "Evaluation of Antenna Q", *IEEE Transactions on Antennas and Propagation*, Vol. 12, Issue 1, pp. 23 – 27, January 1964.

[80] J. T. Prothro, G. D. Durgin, and J. D. Griffin, "The Effects of a Metal Ground Plane on RFID Tag Antennas", *IEEE Antennas and Propagation Society International Symposium*, July 9 – 14, 2006, pp. 3241 – 3244.

[81] D. M. Dobkin and S. M. Weigand, "Environmental Effects on RFID Tag Antennas", *IEEE MTT-S International Microwave Symposium Digest*, June 12 – 17, 2005, pp. 135 – 138.

[82] P. Foster and R. Burberry, "Antenna Problems in RFID Systems", *IEE Colloquium on RFID Technology*, London, October 25, 1999, pp. 3/1 – 3/5.

[83] M. Hirvonen, J. C.-E. Sten, and P. Pursula, "Platform Tolerant Planar Inverted F-Antenna", *Proceedings of URSI/IEEE XXIX Convention on Radio Science*, Espoo, Finland, November 1 – 2, 2004, pp. 47 – 50.

[84] J. C.-E. Sten and M. Hirvonen, "Decay of Groundplane Currents of Small Antenna Elements", *IEEE Antennas and Wireless Propagation Letters*, Vol. 4, pp. 82 – 84, 2005.

[85] J. D. Griffin, G. D. Durgin, A. Haldi, and B. Kippelen, "RF Tag Antenna Performance on Various Materials Using Radio Link Budgets", *IEEE Antennas and Wireless Propagation Letters*, Vol. 5, Issue 1, pp. 247 – 250, December 2006.

[86] Confidex Ltd., "Survivor Brochure", Available at www.confidex.fi/fileadmin/user_upload/pdf/Survivor-small.pdf, referenced August 6th, 2008.

[87] H.-W. Son, G.-Y. Choi, and C.-S. Pyo, "Design of Wideband RFID Tag Antenna for Metallic Surfaces", *IEE Electronic Letters*, Vol. 42, No. 5, pp. 263 – 265, March 2006.

[88] K. V. S. Rao, S. F. Lam, and P. V. Nikitin, "Wideband Metal Mount UHF RFID Tag", *IEEE Antennas and Propagation Symposium*, San Diego, CA, June 2008.

[89] M. Hirvonen, K. Jaakkola, P. Pursula, and J. Säily, "Dual-Band Platform Tolerant Antennas for Radio-Frequency Identification", *IEEE Transactions on Antennas and Propagation*, Vol. 54, No. 9, pp. 2632 – 2637, September 2006.

[90] L. Ukkonen, L. Sydänheimo, and M. Kivikoski, "Patch Antenna with EBG Ground Plane and Two-Layer Substrate for Passive RFID of Metallic Objects", *IEEE Antennas and Propagation Society International Symposium*, June 20 – 25, 2004, pp. 93 – 96.

[91] M. Stupf, R. Mittra, J. Yeo, and J. R. Mosig, "Some Novel Design for RFID Antennas and Their Performance Enhancement with Metamaterials", *Microwave and Optical Technology Letters*, Vol. 49, No. 4, pp. 858 – 867, April 2007.

[92] D. Kim, J. Yeo, and J. I. Choi, "Low Profile Platform-Tolerant RFID Tag with Artificial Magnetic Conductor (AMC)", *Microwave and Optical Technology Letters*, Vol. 50, No. 9, pp. 2292 – 2294, September 2008.

[93] L. Ukkonen, L. Sydänheimo, and M. Kivikoski, "A Novel Tag Design Using Inverted-F Antenna for Radio Frequency Identification of Metallic Objects", *IEEE Symposium on Advances in Wired and Wireless Communication*, April 26 – 27, 2004, pp. 91 – 94.

[94] J.-H. Bae, J.-C. Kim, B.-W. Jeon, J.-W. Jung, J.-S. Park, B.-J. Jang, H.-R. Oh, Y.-J. Moon, and Y.-R. Seong, "Analysis of Phase Noise Requirements on Local Oscillator for RFID System Considering Range Correlation", *37th European Microwave Conference 2007*, Munich, Germany, October 2007, pp. 1664 – 1667.

[95] K. Penttilä, L. Sydänheimo, and M. Kivikoski,"Implementation of Tx/Rx Isolation in an RFID Reader", *International Journal of Radio*

*Frequency Identification Technology and Applications*, Vol. 1, No. 1, pp. 74 – 89, 2006.

[96] J.-W. Jung, K.-K. Nae, J. P. Thakur, H.-G. Cho, and J.-S. Park, "Directional Coupler for UHF Mobile RFID Reader", *Microwave and Optical Technology Letters*, Vol. 49, No. 7, pp. 1501 – 1505, July 2007.

[97] W.-K. Kim, M.-Q. Lee, J.-H. Kim, H.-S. Lim, J.-W. Yu, B.-J. Jang, and J.-S. Park, "A Passive Circulator with High Isolation Using a Directional Coupler for RFID", *IEEE MTT-S International Microwave Symposium*, San Francisco, CA, USA, June 11 – 16, 2006, pp. 1177 – 1180.

[98] F. Wei, X. W. Shi, Q. L. Huang, D. Z. Chen, and X. H. Wang, "A New Directional Coupler for UHF RFID Reader", *Microwave and Optical Technology Letters*, Vol. 50, No. 7, pp. 1973 – 1975, July 2008.

[99] W.-K. Kim, W. Na, J.-W. Yu, and M.-Q. Lee, "A High Isolated Coupled-Line Passive Circulator for UHF RFID Reader", *Microwave and Optical Technology Letters*, Vol. 50, No. 10, pp. 2597 – 2600, October 2008.

[100] J.-W. Jung, H.-H. Roh, H.-G. Kwak, M. S. Jeong, and J.-S. Park, "Adaptive TRX Isolation Scheme by Using TX Leakage Canceller at Variable Frequency", *Microwave and Optical Technology Letters*, Vol. 50, No. 8, pp. 2043 – 2045, August 2008.

[101] H.-W. Son, J.-N. Lee, and G.-Y. Choi, "Design of Compact RFID Reader Antenna with High Transmit/Receive Isolation", *Microwave and Optical Technology Letters*, Vol. 48, No. 12, pp. 2478 – 2481, December 2006.

[102] H. Seppä, T. Varpula, P. Pursula, and M. Kiviranta, "WO/2007/006840 RFID Reading Apparatus And Method", *International patent application*, Filed (National priority) July 2005, published January 2007.

[103] A. Safarian, A. Shameli, A. Rofougaran, and M. Rofougaran, "US/2008/0009258 Integrated Blocker Filtering RF Front End", *US patent application*, Filed February 2007, published January 2008.

[104] D. M. Pozar, *Microwave Engineering*, 2nd Edition, John Wiley & Sons, 1998.

[105] P. D. L. Beasley, A. G. Stove, B. J. Reits, and B.-O. As, "Solving the Problems of a Single Antenna Frequency Modulated CW Radar", *Proceedings of IEEE Radar Conference*, 1990, pp. 391 – 395.

[106] A. G. Stove, "Linear FMCW radar techniques", *IEE Proceedings-F*, Vol. 139, No. 5, pp. 343 – 350, October 1992.

[107] W.-T. Kang, I.-S. Chang, and M.-S. Kang, "Reflection-Type Low-Phase-Shift Attenuator", *IEEE Transactions on Microwave Theory Technology*, Vol. 46, No. 7, pp. 1019 – 1021, July 1998.

[108] L. Ukkonen, L. Sydänheimo, and M. Kivikoski, "Read Range Performance Comparison of Compact Reader Antennas for a Handheld UHF RFID Reader", *IEEE International Conference on RFID*, Grapevine, Texas, USA, March 26 – 28, 2007, pp. 63 – 70.

[109] Y. Kim, I.-J. Yoon, and Y. Kim, "Internal Antenna Design of 900 MHz-Band Mobile Radio Frequency Identification System", *Microwave and Optical Technology Letters*, Vol. 49, No. 9, pp. 2079 – 2082, September 2007.

[110] J.-J. Kang, D.-J. Lee, C.-C. Chen, J. F. Whitaker, and E. J. Rothwell, " Compact Mobile RFID Antenna Design and Analysis Using Photonic-assisted Vector Near-field Characterization", *IEEE International Conference on RFID*, Las Vegas, Nevada, USA, April 16 – 17, 2008, pp. 81 – 88.

[111] J. Savolainen, H. Hirvola, and S. Iraji, "Nokia integroi lukimen E61-malliin: EPC-tunnistus tulee pian kännykkään [Nokia Integrated a Reader into its E61 Model: EPC Identification Comes Soon to Mobile Phones]", *Prosessori*, pp. 42 – 43, August 2008.

Series title, number and
report code of publication

VTT Publications 701
VTT-PUBS-701

Author(s)
Pursula, Pekka

Title

# Analysis and Design of UHF and Millimetre Wave Radio Frequency Identification

Abstract

Radio frequency identification (RFID) is an asymmetric radio protocol, where uplink communication (from transponder to reader) is implemented with backscattering modulation. The idea was first demonstrated in the 1940's. One of the first consumer applications of RFID was access control, and key cards based on an inductive near field coupling are widely used even today. The introduction of Schottky diodes to CMOS processes enabled passive RFID, i.e. transponders without a battery, at ultra high frequencies (UHF) with reasonable cost and read range in the end of 1990's. This has opened up new applications and inspired new research on RFID.

This thesis studies the radio frequency (RF) components and general RF phenomena in RFID at UHF and millimetre waves. The theoretical analysis of the radio path reveals that the read range of a passive UHF system is ideally limited by the downlink, i.e. the power transfer from reader to the transponder. However, the architecture of the reader RF front end is critical, because the transmitted signal may couple a significant amount of noise to the receiver, overpowering the faint reflection from the transponder. In the thesis, two adaptive RF front ends are introduced to eliminate the noise coupling from the transmitter.

One of the most critical problems with UHF RFID has been the detuning of transponder antennas on different mounting platforms. The detuning may significantly diminish the read range of the transponder, especially on metal surfaces. In this thesis, two backscattering-based measurement techniques for the transponder antennas are presented. The detuning effect has been studied using these measurement techniques, and a platform tolerantantenna is introduced.

RFID at millimetre waves enables miniaturisation of the reader antenna, and widening the data bandwidth over short distances. This could be used to access wirelessly mass memories with wide data bandwidth. A semipassive or active transponder could communicate, e.g., with automotive radars. The millimetre wave identification (MMID) has been theoretically studied and experimentally verified at 60 GHz.

ISBN
978-951-38-7133-8 (soft back ed.)
978-951-38-7134-5 (URL: http://www.vtt.fi/publications/index.jsp)

Series title and ISSN
VTT Publications
1235-0621 (soft back ed.)
1455-0849 (URL: http://www.vtt.fi/publications/index.jsp)

Project number
25336

Date
December 2008

Language
English, Finnish abstr.

Pages
82 p. + app. 51 p.

Name of project

Commissioned by
The Finnish Foundation for Technology Promotion (TES), The Foundation of The Finnish Society of Electronics Engineers (EIS), The Espoo Culture Foundation

Keywords
radio frequency identification, RFID, ultra high frequency, UHF, millimetre, waves, millimetre wave identification, MMID, antenna, scattering, backscattering modulation, scattering measurement, reader device, adaptive rf front end

Publisher
VTT Technical Research Centre of Finland
P.O. Box 1000, FI-02044 VTT, Finland
Phone internat. +358 20 722 4520
Fax +358 20 722 4374

Julkaisun sarja, numero ja raporttikoodi

VTT Publications 701
VTT-PUBS-701

Tekijä(t)
Pursula, Pekka

Nimeke

# UHF- ja millimetriaaltoalueen radiotunnistusjärjestelmien tutkimus ja suunnittelu

Tiivistelmä

Radiotunnistus (RFID) on lyhyen kantaman radioprotokolla, jossa yksinkertaisen tunnisteen muisti voidaan lukea langattomasti lukijalaitteen avulla. Tiedonsiirto tunnisteesta lukijalaitteeseen perustuu tunnisteen takaisinsironnan moduloimiseen. Tekniikka on osoitettu kokeellisesti toimivaksi jo 1940-luvulla. Radiotunnistuksen ensimmäisiä kuluttajasovelluksia on induktiivisiin kulkukortteihin ja lukulaitteisiin perustuva kulunvalvonta, jota käytetään tänäkin päivänä yleisesti. Passiivisten, eli paristottomien, tunnisteiden valmistaminen UHF-taajuusalueelle halpeni merkittävästi 1990-luvulla, kun Schottky-diodi integroitiin onnistuneesti CMOS-prosessiin.

Tässä väitöskirjassa on tutkittu radiotunnistusjärjestelmien radiotaajuisia komponentteja ja ilmiöitä UHF- ja millimetriaaltoalueella. Teoreettisen analyysin perusteella tehonsyöttö lukijalta tunnisteelle rajoittaa passiivisen UHF RFID -järjestelmän toimintaetäisyyden noin kymmeneen metriin. Lukijan vastaanottama signaali on tällä etäisyydellä heikko lähettimen kohinaan verrattuna. Tässä väitöskirjassa on esitetty kaksi mukautuvaa radioetuastetta lähettimen kohinan eristämiseksi vastaanottimesta.

Tunnisteantennin sivuunvirittyminen on yleinen ongelma radiotunnistuksessa. Antennin kiinnitysalustan johtavuus tai dielektrisyys muuttaa antennin resonanssitaajuutta, mikä voi estää tunnisteen havaitsemisen. Väitöskirjassa on kehitetty kaksi takaisinsirontaan perustuvaa antennimittausmenetelmää ilmiön tutkimiseksi. Lisäksi työssä esitellään antennirakenne, joka voidaan kiinnittää useille erityyppisille pinnoille antennin toiminnallisuuden heikentymättä.

Millimetriaaltoalueella radiotunnistuksessa voidaan käyttää erittäin laajaa tiedonsiirtokaistaa lyhyillä etäisyyksillä langattoman massamuistin nopeaan lukemiseen. Toisaalta pitkän kantaman sovelluksessa esimerkiksi autotutkia voitaisiin käyttää lukijalaitteina. Väitöskirjassa on tutkittu millimetriaaltojen käyttöä radiotunnistuksessa teoreettisesti sekä osoitettu tekniikan toimivuus kokeellisesti 60 GHz:n taajuudella.

ISBN
978-951-38-7133-8 (nid.)
978-951-38-7134-5 (URL: http://www.vtt.fi/publications/index.jsp)

| Avainnimeke ja ISSN | Projektinumero |
|---|---|
| VTT Publications<br>1235-0621 (nid.)<br>1455-0849 (URL: http://www.vtt.fi/publications/index.jsp) | 25336 |

| Julkaisuaika | Kieli | Sivuja |
|---|---|---|
| Joulukuu 2008 | Englanti, suom. tiiv. | 82 s. + liitt. 51 s. |

| Projektin nimi | Toimeksiantaja(t) |
|---|---|
| | Tekniikan edistämissäätiö (TES), EIS – Elektroniikkainsinöörien seura ry., Espoon seudun kulttuurisäätiö |

| Avainsanat | Julkaisija |
|---|---|
| radio frequency identification, RFID, ultra high frequency, UHF, millimetre, waves, millimetre wave identification, MMID, antenna, scattering, backscattering modulation, scattering measurement, reader device, adaptive rf front end | VTT<br>PL 1000, 02044 VTT<br>Puh. 020 722 4520<br>Faksi 020 722 4374 |

VTT PUBLICATIONS 701

This thesis studies the radio frequency (RF) components and phenomena in radio frequency identification (RFID) at UHF and millimetre waves. The radio path has been theoretically analysed to motivate the experimental work on all the RF components of an UHF RFID system. Two adaptive RF front ends for the reader have been designed and analysed, and an integrated circuit for a passive sensor application is introduced. Two scattering-based measurement techniques for small antennas have been developed, and the techniques have been used in the design and analysis of a platform-tolerant transponder antenna. In addition to UHF, the radio frequency identification at millimetre waves, or millimetre identification (MMID) is discussed. Communication by backscattering modulation is experimentally verified at 60 GHz.

Julkaisu on saatavana

VTT
PL 1000
02044 VTT
Puh. 020 722 4520
http://www.vtt.fi

Publikationen distribueras av

VTT
PB 1000
02044 VTT
Tel. 020 722 4520
http://www.vtt.fi

This publication is available from

VTT
P.O. Box 1000
FI-02044 VTT, Finland
Phone internat. + 358 20 722 4520
http://www.vtt.fi

ISBN 978-951-38-7133-8 (soft back ed.)
ISSN 1235-0621 (soft back ed.)

ISBN 978-951-38-7134-5 (URL: http://www.vtt.fi/publications/index.jsp)
ISSN 1455-0849 (URL: http://www.vtt.fi/publications/index.jsp)

Analysis and Design of UHF and Millimetre Wave Radio Frequency Identification

Pekka Pursula